RESEARCH ARTICLE

Diversity and Distributions WILEY

Gradients of genetic diversity and differentiation across the distribution range of a Mediterranean coral: Patterns, processes and conservation implications

Jean-Baptiste Ledoux[1,2] 🔟 | Raouia Ghanem[3,4] | Mathilde Horaud[2] | Paula López-Sendino[2] | Valèria Romero-Soriano[5] | Agostinho Antunes[1,6] | Nathaniel Bensoussan[2] | Daniel Gómez-Gras[2] | Cristina Linares[7] | Annie Machordom[8] | Oscar Ocaña[9] | José Templado[8] | Raphaël Leblois[10,11] | Jamila Ben Souissi[3,4] | Joaquim Garrabou[2]

[1]CIIMAR/CIMAR, Centro Interdisciplinar de Investigação Marinha e Ambiental, Universidade do Porto, Porto, Portugal

[2]Institut de Ciències del Mar CSIC, Barcelona, Spain

[3]Institut National Agronomique de Tunisie, Université de Carthage, Tunis, Tunisie

[4]Laboratoire de Biodiversité, Biotechnologies et Changements Climatiques (LR11ES09), Université Tunis El Manar, Tunis, Tunisie

[5]Institute of Integrative Biology, University of Liverpool, Liverpool, UK

[6]Departamento de Biologia, Faculdade de Ciências, Universidade do Porto, Porto, Portugal

[7]Departament de Biologia Evolutiva, Ecologia i Ciències Ambientals, Institut de Recerca de la Biodiversitat (IRBIO), Universitat de Barcelona, Barcelona, Spain

[8]Museo Nacional de Ciencias Naturales (MNCN-CSIC), Madrid, Spain

[9]Departamento de Oceanografía Biológica y Biodiversidad, Fundación Museo del Mar de Ceuta, Ceuta, Spain

[10]CBGP, INRAE, CIRAD, IRD, Montpellier SupAgro, University of Montpellier, Montpellier, France

[11]Institut de Biologie Computationnelle, University of Montpellier, Montpellier, France

Correspondence
Jean-Baptiste Ledoux, CIMAR/CIIMAR, Terminal do Cruzeiros do Porto de Leixões, Av. General Norton de Matos, s/n, 4450-208 Porto, Portugal.
Email: jbaptiste.ledoux@gmail.com

Funding information
JBL was funded by a Postdoctoral Grant (SFRH/BPD/74400/2010) from the Portuguese Foundation for Science and Technology (FCT). This research was supported by national funds through FCT within the scope of UIDB/04423/2020 and UIDP/04423/2020 and by the MIMOSA project funded by the Foundation Prince Albert II Monaco. JG, DGG and PL acknowledge the funding of the Spanish government through the "Severo Ochoa Centre of Excellence" accreditation (CEX2019-000928-S). This work was partially supported by the European Union's Horizon 2020 research and innovation

Abstract

Aim: How historical and contemporary eco-evolutionary processes shape the patterns of genetic diversity and differentiation across species' distribution range remains an open question with strong conservation implications. Focusing on the orange stony coral, *Astroides calycularis*, we (a) characterized the pattern of neutral genetic diversity across the distribution range; (b) gave insights into the underlying processes; and (c) discussed conservation implications with emphasis on a national park located on a hotspot of genetic diversity.

Location: South Mediterranean Sea and Zembra National Park.

Methods: We combined new data from 12 microsatellites in 13 populations located in the Centre and in the Western Periphery of the distribution range with a published dataset including 16 populations from the Western and Eastern Peripheries. We analysed the relationship among parameters of genetic diversity (H_e, $Ar_{(g)}$) and structure (population-specific F_{ST}) and two measures of geographic peripherality. We

compared two estimators of pairwise genetic structure (G_{ST}, D_{EST}) across the distribution range. The evolutionary and demographic history of the populations following the Last Glacial Maximum was reconstructed using approximate Bayesian computations and maximum-likelihood analyses. We inferred the contemporary connectivity among populations from Zembra National Park and with the neighbouring area of Cap Bon.

Results: We demonstrate a decrease in genetic diversity and an increase in genetic differentiation from the Centre to the Eastern and Western Peripheries of the distribution range. Populations from Zembra show the highest genetic diversity reported in the species. We identified a spillover effect towards Cap Bon.

Main conclusions: The patterns of genetic diversity and differentiation are most likely explained by "the postglacial range expansion hypothesis" rather than the "central–peripheral hypothesis." Enforcement of conservation measures should be considered to protect this genetic diversity pattern, in particular when considering the low effective population size inferred at many sites.

KEYWORDS

central–peripheral hypothesis, coral, genetic gradient, marine protected area, Mediterranean Sea, postglacial range expansion hypothesis

1 | INTRODUCTION

Genetic diversity is at the heart of populations' resilience and evolutionary potential (Fisher, 1930). Genetic diversity is in direct, reciprocal and complex interactions with higher levels of biological diversity from species (e.g. Reusch et al., 2005) to ecosystem (e.g. Post & Palkovacs, 2009) (see Randall Hughes et al., 2008; Kokko et al., 2017; Pelletier et al., 2009; Schoener, 2011).

Across species' distribution ranges, contemporary patterns of genetic diversity are modelled by the interplay among different eco-evolutionary processes such as genetic drift, gene flow, natural selection, survival and reproduction (e.g. Aurelle et al., 2011, Cahill et al., 2017; Ledoux et al., 2010, 2020). These processes are deeply influenced by the spatial distribution and size of populations, which fluctuate over time in response to historical and contemporary biotic and abiotic factors. While negative gradients of neutral genetic diversity from central to peripheral populations were reported in various species (see Eckert et al., 2008; Hampe & Petit, 2005; Pironon et al., 2017), the underlying processes are still a matter of debate (Guo, 2012; Hardie & Hutchings, 2010). Two non-mutually exclusive hypotheses involving contemporary versus historical processes are usually considered to explain these negative gradients. Following the "*central–peripheral hypothesis*" (Sagarin & Gaines, 2002), the genetic diversity should decline from the centre towards the peripheries of a species' range in response to demo-genetic stochasticity (e.g. low effective size and low connectivity) linked to the environmental characteristics (e.g. spatial isolation and extreme environment) of peripheral habitats (e.g. Johansson et al., 2006). On the other hand, the "*postglacial range expansion hypothesis*" suggests that

historical processes such as serial founder event recolonization (see Austerlitz et al., 1997, 2000; Slatkin & Excoffier, 2012) following the Last Glacial Maximum (LGM 24–18,000 years ago; Lambeck & Purcell, 2005) shape negative genetic gradients from the source to the edge of the expansion range. This pattern is mainly driven by an increase in genetic drift along the axis of expansion due to contrasted demographic histories when comparing peripheral versus central populations. Deciphering the relative impact of these processes on the current patterns of diversity is challenging, relying mainly on the evaluation of historical influences (Eckert et al., 2008; Guo, 2012). However, this is a critical step to build on relevant conservation plan (Frankham, 1995; Hampe & Petit, 2005; Riginos et al., 2019).

Marine protected areas (MPAs) are an efficient tool to preserve genetic diversity and to mitigate the impacts of global change (Roberts et al., 2017). In many cases MPAs are designed following opportunistic rather than scientific criteria, leading to important mismatches between the protected area and the components of biological diversity (e.g. genetic diversity) to protect (Mouillot et al., 2011). With few exceptions (e.g. Arizmendi-Mejía, Linares, et al., 2015; Dalongeville et al., 2018; Gazulla et al., 2021), genetic diversity and related processes are barely considered even though they are crucial for an effective functioning of the protected area (Palumbi, 2004). Among the key eco-evolutionary processes impacting the success of conservation strategies, connectivity within MPAs and among MPAs and neighbouring unprotected areas received particular attention (Magris et al., 2018; Manel et al., 2019). Indeed, the homogenizing effect of connectivity should counterbalance the disruptive effect of genetic drift induced by population depletion, allowing the maintenance and replenishment of genetic diversity.

The identification of populations in terms of their contribution to the connectivity of a network of populations is thus an important step to improve the management of MPAs (e.g. Gazulla et al., 2021; Lukoschek et al., 2016).

The Mediterranean orange stony coral, *Astroides calycularis* (Pallas, 1776), is an azooxanthellate scleractinian mainly found in rocky shallow habitats from the surface to about 40 to 60 m depth (Ocaña, 2012; Terrón-Sigler et al., 2016). While Quaternary fossils were recorded in the Northern Mediterranean (Zibrowius, 1980), the current established distribution range of *A. calycularis* is nearly linear, restricted in width to areas with minimum winter temperatures between 14 and 15°C (mean February temperature), extending from the neighbouring Atlantic Ocean to South Italy along the South-Western Mediterranean (Ocaña et al., 2015; Zibrowius, 1995; Figure 1). This coral is considered as warm-water species (Grubelić et al., 2004; Bianchi, 2007; Prada et al., 2019 but see Movilla et al., 2016), but some populations were recently reported in the eastern Adriatic and in Northern Italy (Bianchi, 2007; Kružić et al., 2002; Teixidó et al., 2020; Figure 1). Whether these atypical populations (i.e. outside of the currently accepted distribution range; Bianchi, 2007) result from species distribution expansion (Bianchi, 2007; Zibrowius, 1995) is still a matter of debate (Casado-Amezúa et al., 2012). Although it has been included in the annex II of the CITES and considered as vulnerable under Bern and Barcelona conventions (Templado et al., 2004), *A. calycularis* appears as least concern species in the IUCN red list due to the demographic stability

of the populations and a relatively high abundance in the South-Western Mediterranean basin (Ocaña, 2012; Ocaña et al., 2009, 2015; Otero et al., 2017).

Astroides calycularis is a gonochoric and brooding species characterized by internal fertilization occurring between April and May with larval release in June (Goffredo et al. 2010; Pellón & Badalamenti, 2016). A first assessment of the spatial pattern of genetic structure was conducted based on mitochondrial (COI) and nuclear (ITS) polymorphisms among 12 populations sampled in Western (i.e. Alboran Sea) and Eastern (i.e. Tyrrhenian Sea) Peripheries of the distribution range of the species (Figure 1). A slight genetic differentiation was observed between the two regions most likely explained by the low polymorphisms of the genetic markers (Merino-Serrais et al., 2012). Using 13 microsatellites and 16 populations, including most of the populations from Merino-Serrais et al. (2012) demonstrated a significant genetic differentiation when considering populations separated by more than 1 km and with $F_{ST} > 0.01$. The genetic differentiation was correlated with geographic distance among populations following a pattern of isolation by distance (IBD). In addition, populations were grouped in different hierarchical genetic clusters in accordance with the regions and the two seas (i.e. Alboran and Tyrrhenian) under survey. These results combined with first-generation migrant analyses confirmed the restricted dispersal capacity of the species as expected from the short demersal larval phase (Casado-Amezúa et al., 2012). The occurrence of local differentiation among populations was recently confirmed
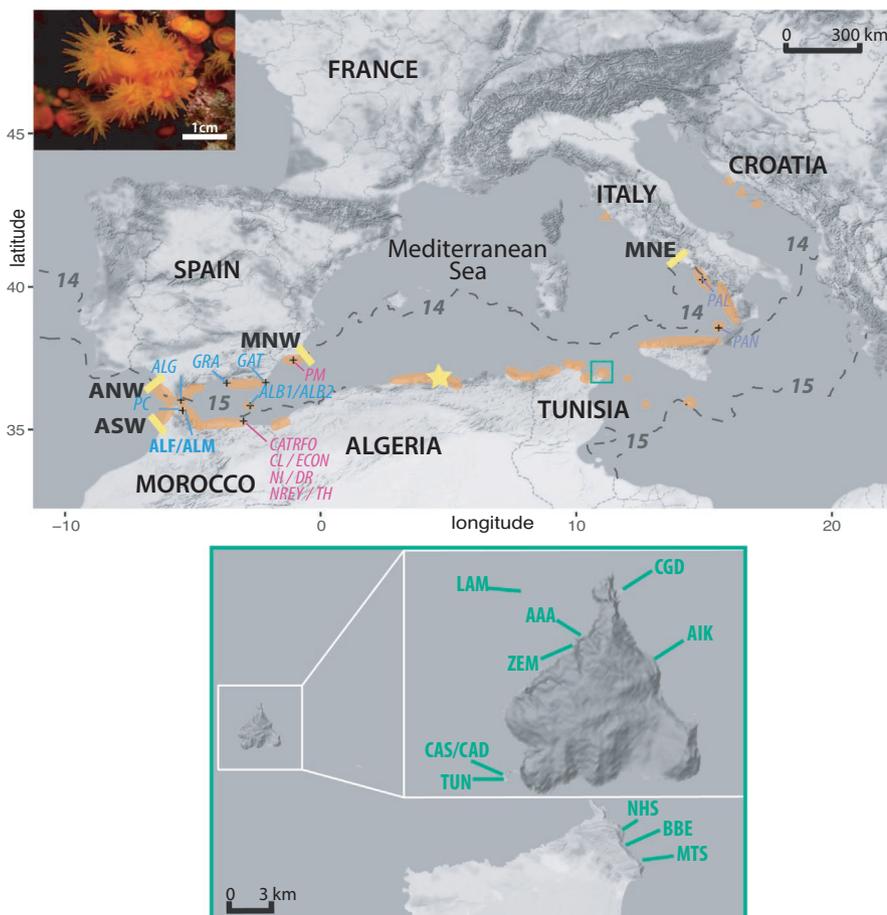

FIGURE 1 The established distribution range of *Astroides calycularis* (orange) is highly restricted in width to areas with minimum winter temperatures between 14 and 15°C (mean February temperature) (Ocaña et al. 2015; Zibrowius, 1995). Orange triangles correspond to atypical populations recently discovered (Bianchi, 2007; Kružić et al., 2002). The yellow star shows the hypothetical range distribution centre (DC). The four yellow lines correspond to the four range limits considered in this study: i) the Atlantic North-Western limit (ANW), the Atlantic South-Western limit (ASW), the Mediterranean North-Western limit (MNW) and the Mediterranean North-Eastern limit (MNE). Studied populations are shown in blue, green and pink and purple according to the results of the clustering analyses (see Results and Figure 4). Populations from Casado-Amezúa et al. (2012) are shown in italics, while populations sampled in this study are shown in bold. Abbreviations of all the populations studied are shown in Table 1

TABLE 1 Characteristics of the samples. For each sample, the location within the distribution range, the locality of origin, the sample name, the coordinates and the depth and number of sampled individuals are given

Distribution range	Region	Sample name	latitude (°N)	longitude (°E)	Depth (m)	Number of individuals
Western margin	Algeciras	ALG	36.11148	−5.414777	not mentioned	25
	Ceuta	PC	35.895813	−5.279909	not mentioned	25
	Ceuta	ALF	35.900772	−5.278116	25	36
	Ceuta	ALM	35.900773	−5.278115	1–2	40
	Granada	GRA	36.728306	−3.693984	not mentioned	20
	Alboran Island	ALB2	35.948148	−3.04062	not mentioned	18
	Alboran Island	ALB1	35.94952	−3.038359	not mentioned	24
	Cap Tres Forcas	CATFR	35.432017	−2.992924	not mentioned	29
	Congreso Island	CL	35.177622	−2.444003	not mentioned	22
	Congreso Island	ECON	35.177776	−2.439487	not mentioned	22
	Isabel II Island	NI	35.183446	−2.429337	not mentioned	20
	Isabel II Island	DR	35.181334	−2.426457	not mentioned	24
	Rey Francisco Island	TH	35.18151	−2.423263	not mentioned	22
	Rey Francisco Island	NREY	35.184825	−2.423081	not mentioned	22
	Cabo de Gata	GAT	36.708456	−2.1988	not mentioned	23
	Portman Bay	PM	37.577925	−0.842663	not mentioned	31
Centre	Zembra National Park	CAD	37.119105	10.787799	8	10
	Zembra National Park	CAS	37.119106	10.7878	1	12
	Zembra National Park	TUN	37.11757	10.789065	1	13
	Zembra National Park	LAM	37.141345	10.795576	15–17	11
	Zembra National Park	ZEM	37.135534	10.800877	2–5	36
	Zembra National Park	AAA	37.136412	10.80194	2–5	16
	Zembra National Park	CGD	37.142209	10.806703	10	24
	Zembra National Park	AIK	37.130744	10.81443	5–7	24
	Eastern Cap Bon	NHS	37.072771	11.060529	6	16
	Eastern Cap Bon	MTS	37.064735	11.061806	3	18
	Eastern Cap Bon	BBE	37.05896	11.067047	6–8	18
Eastern margin	Panarea Island	PAN	38.633105	15.069237	not mentioned	24
	Palinuro	PAL	40.02844	15.267492	not mentioned	30

Note: CAS and CAD corresponded to the same location but were sampled at different depths. Light grey samples are those from Casado-Amezúa et al. (2012).

using transcriptomic data (Teixidó et al., 2020). While these studies greatly improved our knowledge regarding the ecology of *A. calycularis*, they were mainly focused on populations located at the Eastern and Western Peripheries. Whether those genetic patterns can be generalized to the Centre of the species range remains an open question with critical implication for the species' conservation.

The main objective of the study was to characterize the spatial pattern of genetic diversity in *A. calycularis* at two contrasted spatial scales. First, we considered most of the species distribution range and provided insights into the relative impact of contemporary ("central–peripheral hypothesis") versus historical ("postglacial range expansion hypothesis") processes on the pattern of genetic diversity. Then, we deciphered the functioning of the Zembra National Park

off the Tunisian coast, which harbour dense populations of *A. calycularis* (Boudouresque et al., 1986; Ghanem et al., 2019, 2021). More particularly, we sampled and genotyped 13 populations from two parts (Centre vs. Western Periphery) of *A. calycularis'* distribution range. Combining these data with the dataset of Casado-Amezúa et al. (2012), which covered Western and Eastern range peripheries, we: i) characterized the spatial pattern of genetic diversity across the species' distribution range; ii) reconstructed the species evolutionary and demographic history to test for the impact of historical processes on the observed pattern. Then, focusing on the Zembra National Park, we: iii) identified important populations for the network of connectivity; and iv) characterized the interactions with populations located outside of the National Park. We discussed the

implications of these results for the conservation of the species and for the management of the Zembra National Park.

2 | METHODS

2.1 | Sampling and datasets

Five to ten polyps of ten to 40 *A. calycularis* colonies from 13 populations from the northern coast of Africa were collected by SCUBA diving. Two populations were sampled in Ceuta (Spain) at the current Western Periphery of the species range. The remaining 11 populations were sampled in Tunisia and were considered as Centre populations (see measure of peripherality below). From these Tunisian populations, eight belong to the National Park of Zembra and three were collected outside the National Park on the coast of Cap Bon (Figure 1; Table 1). Sampling was conducted at depths from 1 to 17 metres in 2017. The resulting 336 fragments were conserved in 95% ethanol and stored at −20°C prior to DNA extraction.

DNA extraction, microsatellite genotyping and quality check are described in Appendix S1. Following the quality check, 274 of the 336 fragments were retained.

In order to combine these 274 genotypes with the dataset from Casado-Amezúa et al. (2012), including 16 populations sampled on the Western and Eastern Peripheries and genotyped with the same set of 12 microsatellites, we standardized the allele scoring based on the comparison of allele frequencies in three populations (ALF, ALM and PC; Table 1, Figure 1). These three populations were sampled in the same location among the two studies (Appendix S2). The final dataset included 655 individuals from 29 populations genotyped with 12 microsatellites (Figure 1; Table 1). Considering the bathymetric range of the species and given that the sea level of the Mediterranean was 120m lower than it is today during the Last Glacial Maximum (24–18,000 years ago; Lambeck & Purcell, 2005), we considered that all these populations were recolonized since the LGM. Frequencies of null alleles were estimated for each locus and sample using in FREENA (Chapuis & Estoup, 2007). GENETIX 4.05 (Belkhir et al., 2004) was used to compute the f, the Weir and Cockerham (1984) estimator of F_{IS}, and to test for linkage equilibrium for each pair of loci overall populations and in each population, using 1,000 permutations.

2.2 | Spatial genetic structure

We performed a clustering analysis with STRUCTURE 2.2 (Pritchard et al., 2000) and a discriminant analysis of principal components (DAPC, Jombart et al., 2010) in ADEGENET (Jombart, 2008). The two analyses are described in Appendix S3.

Genotypic differentiation among populations was quantified using the Weir and Cockerham (1984) estimator of F_{ST}, θ, and tested using an exact test (Raymond & Rousset, 1995) with default

parameters in GENEPOP 4.7 (Rousset, 2008). Isolation-by-distance (IBD) pattern was analysed through the correlation of genetic and geographic distances among populations (Rousset, 1997) but considering only the 11 populations from Tunisia due to the sampling gap between the Western Periphery and Centre populations. The significance of the correlation between the genetic distances ($F_{ST}/(1–F_{ST})$) and the logarithms of geographic distances (Ln(d)) was tested by the Mantel test with 10,000 permutations in GENEPOP. Geographic distances were estimated following the most direct path among populations along the coastline in Google Earth (http://earth.google.com). We estimated the "neighbourhood size" as the inverse of the slope of the linear regression between $F_{ST}/(1–F_{ST})$ and Ln(d) (Rousset, 1997).

2.3 | Patterns of genetic diversity and structure over the distribution range accounting for geographic peripherality

We estimated the gene diversity, H_e (Nei, 1973), in GENETIX 4.05 and computed the allelic richness ($Ar_{(10)}$) in ADZE (Szpiech et al., 2008) using the rarefaction method (Petit et al., 1998) with the minimum of 10 genes at a locus in a population. GESTE (Foll & Gaggiotti, 2006) was used to compute the population-specific F_{ST}, as an estimate of the relative impact of genetic drift on the differentiation of the considered population (Gaggiotti & Foll, 2010). To characterize the pattern of genetic diversity and structure over the distribution range, we plotted H_e, $Ar_{(10)}$ and the population-specific F_{ST}s function of the longitude of the samples. Following a visual inspection of the data, we conducted a cubic regression to fit the curvilinear relationship among the variables (see Guo, 2012).

Bearing in mind the shape of the distribution range with multiple range limits (Figure 1), we complemented this approach following Yakimowski and Eckert (2007). We measured the relative geographic periphery of these populations based on two measures of the peripherality. First, we defined a hypothetical geographic centre of the current distribution range (DC) by estimating the coordinates of the geographic centre between the Eastern (40.803785°N; 13.431352°E) and Atlantic South-Western Peripheries (35.779586°N; 5.932594°E). Considering the coastal habitat of the species, we kept the longitude coordinate and translated this midpoint to the nearest coast (36.887534°N; 4.821389°E; Figure 1). This centre was defined based only on geographic (and not ecological) considerations, and accordingly, it is hypothetical. For each sample, we estimated the geographic distance to DC following the coastline in accordance with the isolation-by-distance pattern (see Casado-Amezúa et al., 2012 and Results). For island populations (e.g. LAM, ZEM), we took the shortest distance to the main coast.

The second measure of geographic peripherality reflects the distance to the nearest current range limit (DNRL) following the coastline. Following Bianchi (2007), Ocaña et al. (2015) and Zibrowius

(1995), we considered four range limits: the Atlantic North-Western limit (ANW; 36.515868°N; 6.292235°E), the Atlantic South-Western limit (ASW; 35.779586°N; 5.932594°E), the Mediterranean North-Western limit (MNW; 37.636409°N; 0.687187°E) and the Mediterranean North-Eastern limit (MNE; 40.803785°N; 13.431352°E) (Figure 1). Eastern and Southern range limits imposed by the Western coast of Italy and the Northern coast of Africa were not considered.

These two measures are complementary, capturing different aspects of peripherality. For instance, the Tunisian populations, considered here as Centre populations, are shifted from the hypothetical Centre (DC), showing a distance to the Centre only slightly lower than some populations from the Western Periphery (e.g. NREY, TH and DR). However, their distances to the nearest range limit (DNRL) are at least two times higher than the distances estimated for the populations from the Eastern and Western Peripheries.

To characterize the spatial pattern of genetic diversity, we tested the significances of the slopes of the linear regressions among the two estimators of genetic diversity (H_e and $Ar_{(10)}$), the estimate of genetic structure (population-specific F_{ST}) and the two measures of the geographic peripherality (DC and DNRL) using a permutation procedure ($n = 10,000$) in R (R Core Team, 2021).

2.4 | Comparison of the pairwise differentiation among populations from the Centre and the Peripheries of the distribution range

We used GENODIVE (Meirmans & vanTienderen, 2004) to compute and compare two measures of genetic differentiation quantifying complementary aspects of population structure (Jost et al., 2018): the nearness to fixation, G_{ST} (Nei, 1987), and the relative degree of allelic differentiation, D_{EST} (Jost, 2008). We first compare the global measures (global G_{ST} vs. global D_{EST}) to gain insights into the spatial distribution of alleles following Jost et al. (2018). Then, we regressed pairwise G_{ST}s on pairwise D_{EST}s. This allowed to compare the nearness to fixation for population pairs showing the same level of allelic differentiation and, accordingly, to test for a potential increase in genetic fixation from the Centre to the Peripheries of the distribution range. Two sets of regression analyses were conducted. In the first set, we compared the relationship among G_{ST}s and D_{EST}s considering a "dataset" variable (i.e. dummy variable), which included two categories of population pairs: two populations from the same periphery or two populations from the centre. In order to account only for these two categories of population pairs, this first set of analyses was focused on $-0.1 < D_{EST}$s < 0.4. In the second set, we compared the G_{ST}s D_{EST}s relationship considering a "dataset" variable (i.e. dummy variable) including three categories of population pairs: the two populations from different peripheries, one population from the Centre versus one from the Eastern Periphery or one population from the Centre versus one from the Western Periphery. Here, the analysis was restricted to $0.55 < D_{EST}$s < 0.85. In each set, we fitted a multiple regression model including the "dataset"

variable. We tested for the differences among the regression slopes of each category by looking at the significance of the D_{EST} x "dataset" interaction.

2.5 | Influence of historical processes: evolutionary and demographic history

Following the postglacial range expansion hypothesis, centre to periphery negative gradients in genetic diversity (see Results) should result from an imprint of serial founder events. In this framework, the current peripheral populations are assumed to be farther from the ancestral population than the central populations. We thus expect an increase in genetic drift along the recolonization axis resulting in contrasted demographic histories among the current central versus peripheral populations. Current peripheral populations should be impacted by stronger founder effects with more recent foundation time compared with current central populations. Note that owing to the variations of the sea level in the Mediterranean during the Last Glacial Maximum (LGM), the ancestral population was most likely not located at the hypothetical geographic centre of the current distribution range (DC). To test the postglacial range expansion hypothesis, we inferred the evolutionary scenario leading to the observed pattern of genetic diversity using an approximate Bayesian computation (ABC) analysis implemented in DIY-ABC 2.0.4 (Cornuet et al., 2014, 2010). In the present case and considering computation limitations due to the number of populations (29), we aimed to characterize and compare the dynamics of the recolonization among the four main genetic sub-clusters identified with STRUCTURE (see Results): the South-East Italian sub-cluster from the Eastern Periphery, and the Spanish sub-cluster and the South Alboran sub-cluster, both from the current Western Periphery and the Tunisian sub-cluster, which is assumed to be central based on the measures of peripherality. We compared five different evolutionary scenarios (Figure 2). Briefly, in Scenario 1 we considered a simultaneous divergence of the four sub-clusters from the ancestral population. Scenario 2 simulated a secondary contact between the sub-clusters from the Eastern and Western Peripheries resulting in the Tunisian sub-cluster. For Scenarios 3, 4 and 5, we stimulated different sequential recolonization scenarios with the oldest divergent event involving the Tunisian sub-cluster (Scenario 3), the sub-clusters from the Western Periphery (Scenario 4) or the South-East Italian sub-cluster (Scenario 5). Those scenarios along with the retained summary statistics and the different steps of the analyses are described in Table 2 and Appendix S4.

We characterized the demographic history of each of the 29 populations using the model of a panmictic population with single past variation in population size (Model OnePopVarSize, Leblois et al., 2014), implemented in MIGRAINE (http://kimura.univ-montp2.fr/~rousset/Migraine.html; Rousset et al., 2018). We choose to consider a discrete, and not the default exponential, change in population size. The model has three canonical parameters: the current
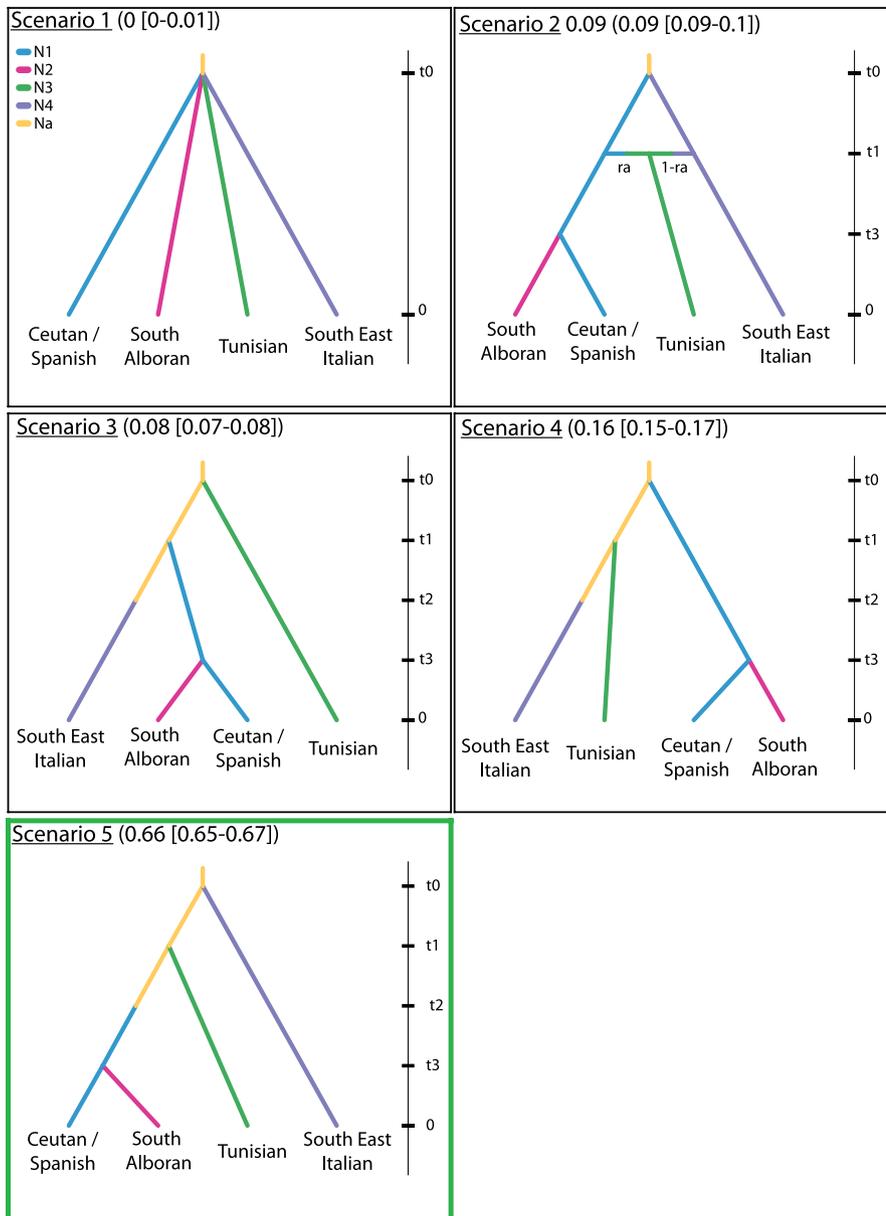
FIGURE 2 Five different scenarios were considered in the ABC analyses to reconstruct the evolutionary history of *A. calycularis*. *N* and *t* values correspond to population size and to timing in divergence events, respectively (time is not scaled). The retained scenario is surrounded in green. Posterior probability and corresponding 95% confidence interval of each scenario are shown

scaled population size ($\theta_{cur} = 2*N*\mu$) the scaled time T ($T = T_g/2N$) at which the size change occurred, and the ancestral scaled population size ($\theta_{anc} = 2*N_{anc}*\mu$), with μ corresponding to the mutation rate per locus per generation, N and N_{anc} to the current and ancestral population sizes expressed in numbers of genes (i.e. "haploid" population sizes), and T_g to the time in generations. As we considered a generalized stepwise mutation model (*GSM*), there is an additional fourth canonical parameter: pGSM, the parameter of the geometric distribution of mutation steps. Those parameters are inferred from the data using the class of coalescent-based importance sampling algorithms (Iorio & Griffiths, 2004a, 2004b; Leblois et al., 2014; Rousset et al., 2018). The detection of past change in population size is based on the analysis of the N_{ratio} composite parameter, the ratio of current over ancestral population sizes ($N_{ratio} = N_{cur}/N_{anc}$). A N_{ratio} >1 corresponds to a population expansion and a N_{ratio} <1 to a contraction. Details of each MIGRAINE run (number of trees, points and iterations) are shown in Appendix S5.

2.6 | Connectivity in Zembra National Park and neighbourhood populations

We inferred the connectivity among populations within the Zembra National Park and between the Park and the populations situated along the coast of Cap Bon. We conducted a filtered assignment analysis following Lukoschek et al. (2016) using Geneclass 2.0 (Piry et al., 2004). We conducted a first-generation migrant (FGM) analysis using the Bayesian criteria of Rannala and Mountain (1997) simulating 100,000 individuals and a type 1 error (alpha) of 0.005. Identified FGMs were removed from the dataset. In a second step, those FGMs were assigned to the reference dataset (i.e. without FGMs). In the last step, we considered a FGM to be assigned to a particular population when the assignment probability was higher than 0.01. Multiple assignments were allowed. When the assignment probability was lower than 0.01 for all populations, the migrant was considered as coming from an unsampled population.

TABLE 2 Prior (uniform; UN) and posterior distributions of demographic (*N*), historical (*t*) and admixture rate (*ra*) parameters used in the ABC analysis. The posterior distributions of the different parameters were estimated considering Scenario V. The mode, 95% confidence intervals and relative median of the absolute error (RMAE) of each parameter are shown. N1: Spanish sub-cluster; N2: South Alboran sub-cluster; N3: Tunisian sub-cluster; N4: South-East Italian sub-cluster; Na: Ancestral population

Parameter	Prior distribution [Lower bound; Upper bound]	Posterior distribution summary			
		Mode	q025	q975	RMAE
N1	UN [10; 20,000]	15,500	3,700	19,600	0.235
N2	UN [10; 20,000]	2,860	763	17,400	0.252
N3	UN [10; 40,000]	13,300	5,470	35,100	0.208
N4	UN [10; 40,000]	10,200	4,100	30,900	0.196
Na	UN [10; 5,000]	402	90,7	4,740	0.404
t3	UN [10; 8,000]	1,300	242	5,270	0.350
t2	UN [10; 8,000]	4,580	1,220	7,770	0.212
t1	UN [10; 40,000]	22,100	8,560	38,200	0.280
t_0	UN [10; 50,000]	40,400	16,300	49,300	0.190
ra	UN [0.001; 0.999]				
μ	UN [$1*10^{-4}$; $1*10^{-3}$]	$1*10^{-4}$	$1.01*10^{-4}$	$3.44*10^{-4}$	0.241
P_{GSM}	UN [$1*10^{-1}$; $9*10^{-1}$]	0.115	0.112	0.858	0.336
P_{SNI}	UN [$1*10^{-8}$; $1*10^{-5}$]	$1.09*10^{-08}$	$1.14*10^{-8}$	$7.1*10^{-6}$	3.493

For multiple tests, all significance levels were corrected using a false discovery rate (FDR) correction (Benjamini & Hochberg, 1995).

3 | RESULTS

3.1 | Hardy–Weinberg equilibrium, genetic diversity and differentiation over the distribution range

Significant linkage disequilibrium was detected for two pairs of loci when considering all the populations: *Ac-10* and *Ac-37* and *Ac-18* and *Ac-34*. Linkage disequilibrium was detected in ALM (*Ac-34 Ac-37*), CAD (*Ac-25 Ac-37*), ALG (*Ac-10 Ac-37*), ALB2 (*Ac-10 Ac-37* and *Ac-22 Ac-7E*) and PAL (*Ac-10 Ac-37* and *Ac-11 Ac-7*). Most of these populations were also characterized by very low effective population size or significant departure from panmixia (see below). When these five populations were discarded from the dataset, non-significant linkage disequilibrium was detected when considering all the populations (not shown). Accordingly, we kept all the microsatellites for downstream analyses. The frequency of null alleles was between 0 for NI and ALM and 0.13 for MTS, BBE and AIK (mean over populations ±SE = 0.05 ± 0.04). Observed heterozygosity values were between 0.23 for PM and 0.69 for AAA (mean over populations ±SE = 0.54 ± 0.09). The gene diversity H_e ranged between 0.29 (PM) and 0.74 (AAA) (mean over populations ±SE = 0.57 ± 0.11). The *f* estimator of F_{IS} varied between −0.013 (ALM) and 0.172 (PM) (mean over populations ±SE = 0.069 ± 0.065), and significant departure from panmixia was observed in nine of the 29 the populations (significant Hardy–Weinberg disequilibrium p-value after FDR correction). The lowest and highest values of $Ar_{(10)}$ were observed for PM (1.92) and AAA (4.60) (mean $Ar_{(10)}$ over populations ±SE = 3.52 ± 0.72).

Population-specific F_{ST}s varied between 0.12 (95% CI: 0.08–0.16) for CAS and 0.52 (95% CI: 0.42–0.62) for PM. Non-overlapping 95% CIs were observed among different populations, particularly when considering populations from the Centre versus Western Periphery (Table 3).

We demonstrated significant curve–linear relationships among H_e, $Ar_{(10)}$ and population-specific F_{ST}s and longitude ($p <.01$). This pattern was complemented by the significant decreases in H_e, $Ar_{(10)}$ and increase in population-specific F_{ST}s with the distance to centre (DC) and the significant increases in H_e, $Ar_{(10)}$ and decrease in population-specific F_{ST}s with the distance to the nearest range limit (DNRL) (Figure 3).

3.2 | Spatial genetic structure

Evanno's method (Evanno et al., 2005) identified two main genetic clusters, with a smaller secondary peak for K = 4 (Appendix S3). The first cluster encompassed all the individuals from the Centre (Tunisian region) and from the Eastern Periphery (Southern East Italian region) with a very high mean membership coefficient (0.99) (Figure 4a). The remaining individuals from the Western Periphery (South Alboran, Ceutan and South-Western Spanish regions) were grouped in a second cluster (0.99). When considering the likelihood of observing the data, (lnP(D)) increased until K = 4, showed a plateau for K = 5 with high standard deviation, slightly increased for K = 6 and, plateaued again for the remaining values (Appendix S3). For K = 3, the first cluster was divided in two sub-clusters segregating the individuals from the Centre (Tunisian sub-cluster, mean membership coefficient = 0.99) from the individuals from the Eastern Periphery (Southern East Italian sub-cluster, mean membership

TABLE 3 Genetic diversity of each sample

	Distance to the nearest range limit (DNRL in km)	Distance to the centre (DC in km)	r	H_e	H_o	$Ar_{(10)}$	f	Population-specific F_{ST} [95% CI]
ALG	119	1,057.86	0.01	0.55	0.56	2.97	−0.02	0.361 [0.28–0.45]
PC	105	1,032	0.04	0.60	0.56	3.48	0.06	0.269 [0.20–0.34]
ALF	104.5	1,031.5	0.03	0.58	0.60	3.37	−0.03	0.28 [0.22–0.34]
ALM	104	1,031	0.03	0.59	0.60	3.33	−0.01	0.31 [0.24–0.38]
GRA	312	1,340	0.02	0.52	0.51	2.83	0.03	0.36 [0.27–0.44]
ALB2	307.26	899.93	0.13	0.54	0.46	3.06	**0.15**	0.329 [0.25–0.41]
ALB1	307	899.67	0.09	0.49	0.49	2.92	0	0.323 [0.24–0.40]
CATRFO	394	845	0.13	0.59	0.56	3.56	0.06	0.214 [0.16–0.27]
CL	472	775.83	0.04	0.46	0.43	2.84	0.06	0.305 [0.23–0.38]
ECON	473.61	774.22	0.1	0.50	0.46	3.11	0.08	0.254 [0.19–0.32]
NI	474.1	773.73	0.08	0.48	0.52	2.8	−0.09	0.32 [0.24–0.40]
DR	474.51	773.32	0.12	0.49	0.50	3.03	−0.03	0.258 [0.19–0.32]
TH	475.05	772.78	0.05	0.46	0.45	3.06	0.03	0.261 [0.20–0.33]
NREY	474.57	773.26	0.05	0.49	0.43	2.88	0.12	0.297 [0.23–0.37]
GAT	203	1,497	0.04	0.46	0.44	2.46	0.03	0.449 [0.36–0.55]
PM	15.8	1681	0.13	0.29	0.23	1.92	**0.17**	0.526 [0.42–0.62]
CAD	1,033.705	728.55	0.02	0.71	0.67	4.36	0.07	0.147 [0.09–0.2]
CAS	1,033.705	728.55	0.03	0.72	0.61	4.59	**0.17**	0.123 [0.08–0.16]
TUN	1,033.475	728.32	0.05	0.70	0.61	4.32	0.13	0.144 [0.10–0.19]
LAM	1,031.675	731.16	0.02	0.72	0.65	4.43	0.11	0.158 [0.11–0.21]
ZEM	1,031.899	730.55	0.04	0.72	0.67	4.44	0.07	0.135 [0.10–0.17]
AAA	1,031.689	730.955	0.05	0.74	0.69	4.6	0.08	0.125 [0.08–0.16]
CGD	1,030.174	731.934	0.06	0.71	0.66	4.48	0.07	0.126 [0.09–0.16]
AIK	1,029	727.62	0.03	0.68	0.58	4.25	**0.12**	0.167 [0.12–0.21]
NHS	1,013	743	0.02	0.66	0.57	4	**0.14**	0.199 [0.14–0.25]
MTS	1,015	725	0	0.63	0.56	3.73	**0.12**	0.244 [0.18–0.31]
BBE	1,016	746	0.03	0.67	0.56	3.93	**0.16**	0.224 [0.17–0.28]
PAN	500	1,246.56	0.06	0.61	0.54	3.63	**0.11**	0.274 [0.21–0.33]
PAL	210	1547	0.07	0.62	0.58	3.76	**0.06**	0.245 [0.19–0.29]

Note: r: frequency of null alleles estimated in FREENA; H_o: observed heterozygosity; H_e: gene diversity (Nei, 1973); f: Weir and Cockerham (1984) estimator of F_{IS} (bold values are significant at 0.01); $Ar_{(10)}$: rarefied allelic richness considering a minimum of 10 genes at a locus in a population; population-specific F_{ST} and 95% confidence intervals. Distances to the nearest range limit and the hypothetical distribution centre are shown. Light grey samples are those from Casado-Amezúa et al. (2012)

coefficient = 0.98). For K = 4, the second cluster was divided into two sub-clusters segregating all the individuals from the Ceutan and the South-Western Spanish regions with the exception of PM (Spanish sub-cluster, mean membership coefficient = 0.91) from individuals from the South Alboran region and PM (South Alboran sub-cluster, mean membership coefficient = 0.90), with individuals from CATRFO showing an admixed pattern (mean membership coefficient = 0.57).

The DAPC analyses supported a geographic imprint in the spatial pattern of genetic structure when considering the first three PCs (Figure 4b). Individuals from the Western Periphery (16 populations) were separated from the remaining individuals sampled in the Centre (11 populations) and Eastern Periphery (2 populations)

of the species range along the first axis. The second axis divided the individuals from the Centre and the Western Periphery from the individuals from Eastern Periphery. A continuum of the populations from the Western Periphery, with CATRFO, ALB1 and ALB2 in intermediate positions, was observed along the third axis. Those three axes represented 95.76% of the total variation in the data.

The exact tests for genotypic differentiation were significant at the global level and for 372 pairwise comparisons (92%; Appendix S6). The remaining 34 non-significant tests involved population pairs from the same genetic sub-cluster with a maximum pairwise geographic distance equal to 4.75 km (AIK vs. TUN).

The global F_{ST} was 0.237. The pairwise F_{ST}s ranged from $−9.4*10^{-3}$ for CAS versus LAM to 0.52 for MTS versus PM (Appendix S6). The

FIGURE 3 Spatial pattern of genetic diversity: (a and b) Cubic regressions of H_e, $Ar_{(10)}$, the population-specific F_{ST} and the longitude of the sampled locations following Guo (2012); (c and d) linear regressions of H_e, $Ar_{(10)}$, the population-specific F_{ST} function of the distance to the nearest range limit (DNRL, km; see Figure 1); (e and f) linear regressions of H_e, $Ar_{(10)}$, the population-specific F_{ST} function of the distance to the centre range (DC, km; see Figure 1). H_e, $Ar_{(10)}$ and the population-specific F_{ST} are shown with circles, triangles and crosses, respectively. In plots (a), (c) and (e), top and down R^2 and p-value correspond to the regressions involving H_e and $Ar_{(10)}$, respectively
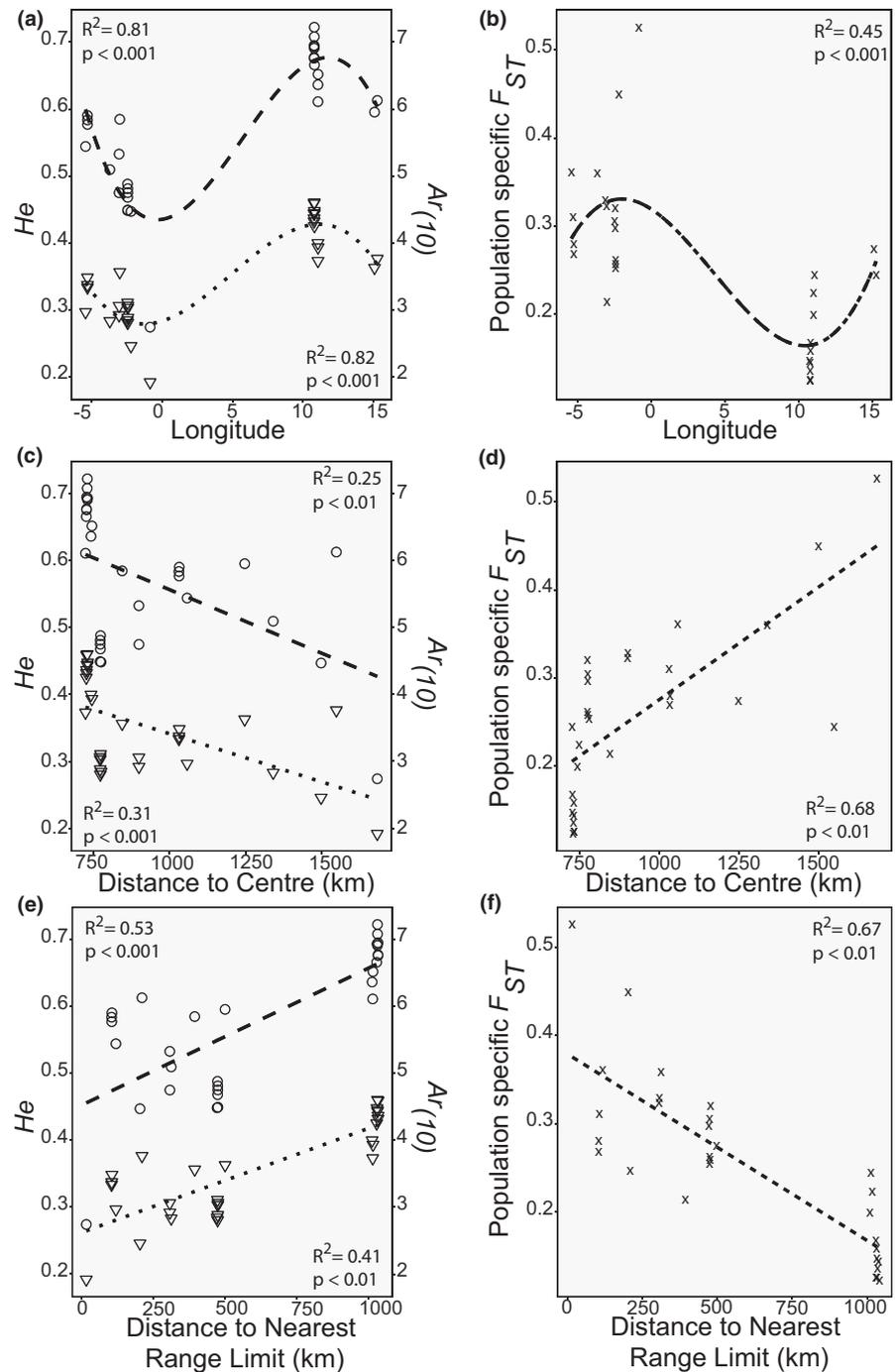
genetic distance ($F_{ST}/(1–F_{ST})$) and the geographic distance ($Ln(d)$) were significantly correlated supporting an IBD pattern among the 11 Centre populations ($p = 3*10^{-4}$). The slope of the regression was 0.011 resulting in a Nb equal to 91 individuals.

The global G_{ST} was 0.235 (95% CI: 0.185–0.288), while the global D_{EST} was 0.436 (95% CI: 0.339–0.542). The pairwise G_{ST}s ranged from $-5*10^{-3}$ for CAS versus AAA to 0.511 for PM versus PAN. The pairwise D_{EST}s ranged between $-1.5*10^{-2}$ for AAA versus CAS and 0.834 for PM versus PAL and PM versus PAN (Appendix S6). Focusing on D_{EST}s from −0.1 to 0.4 (i.e. population pairs involving populations from the Centre or from the same Periphery), the $D_{EST} \times$ "dataset" interaction was significant [$F(1, 172) = 56.8$; $p = 2.6*10^{-12}$] implying

significant differences between the slopes of the two linear regressions. Regarding D_{EST}s from 0.55 to 0.85 (i.e. population pairs involving one central and one peripheral population or two populations from the two peripheries), the interaction $D_{EST} \times$ "dataset" was also significant [$F(2, 224) = 6.96$; $p = 1.1*10^{-3}$] (Figure 5).

3.3 | Evolutionary history

The ABC analysis unambiguously supported Scenario V (posterior probability (95% CI) = 0.66 (0.65–0.67); see Figure 2) corresponding to a sequential foundation of the four different sub-clusters with a
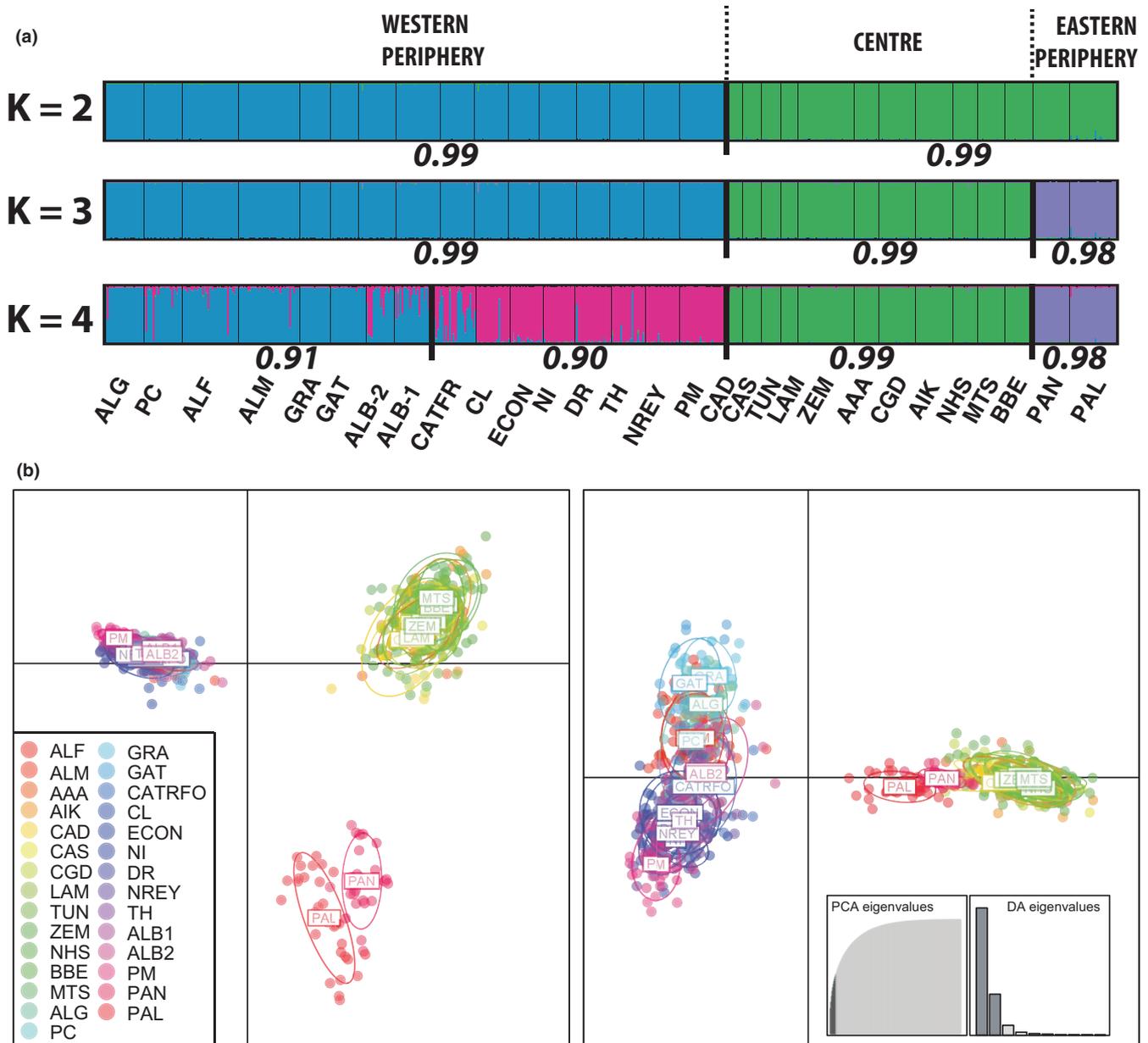
FIGURE 4 Spatial genetic structure: (a) Clustering analysis conducted with STRUCTURE considering $K = 2$, $K = 3$ and $K = 4$. Each individual is represented by a vertical line partitioned in K-coloured segments, which represent the individual membership fraction in K clusters. Thin and thick black vertical lines delineate the different locations and regions, respectively. Samples names and geographic areas are shown below and above the assignment plots (for abbreviations, see Table 1). The mean membership coefficient for each cluster is shown. (b) Scatter plots of the discriminant analysis of principal components (DAPC) based on a *a-score* of 11. The left panel shows the plot corresponding to axes 1 and 2, and the right panel shows the plot corresponding to axes 1 and 3. The three axes represented 95.76% of the total variation in the data. Each dot corresponds to one individual ($n = 655$) from each of the 29 populations, which are represented by different colours. Inertia ellipses centre on the mean for each location and include 67% of the sampling points

first divergence from the ancestral pool of the Southern East Italian sub-cluster (t_0), followed by a divergence of the Tunisian sub-cluster (t_1), and the Spanish (t_2) and the South Alboran (t_3) sub-clusters. The remaining four scenarios showed much lower posterior probabilities: from 0 for Scenario I to 0.16 (95% CI: 0.15–0.17) for Scenario IV. Following a logistic approach and accounting for the five scenarios, the posterior predictive error of scenario choice based on 1,000 simulated datasets was 0.32. Model checking analyses indicated that data simulated under the Scenario V and parameter posterior

distributions fitted well the observed data. None of the 16 summary statistics simulated under Scenario V were significantly different from the observed values. Overall, posterior distributions of demographic parameters for Scenario V were well estimated with peaked posteriors clearly different from prior distributions (not shown). The modes of the posterior distribution of effective population size (in number of diploid individuals) ranged from 2,860 (95% CI: 763–17,400) for the South Alboran sub-cluster to 15,500 (95% CI: 3,700–19,600) for the Spanish sub-cluster. Regarding the ancestral

FIGURE 5 Linear regression among pairwise G_{ST}s (Nei, 1987; nearness to fixation) and D_{EST}s (Jost, 2008; allelic differentiation) considering population pairs: (a) from the same periphery (in orange) or from the Centre (in red); (b) from the Western versus Eastern peripheries (in green), from the Centre versus Western periphery (in blue) and from the Centre versus Eastern periphery (in purple)
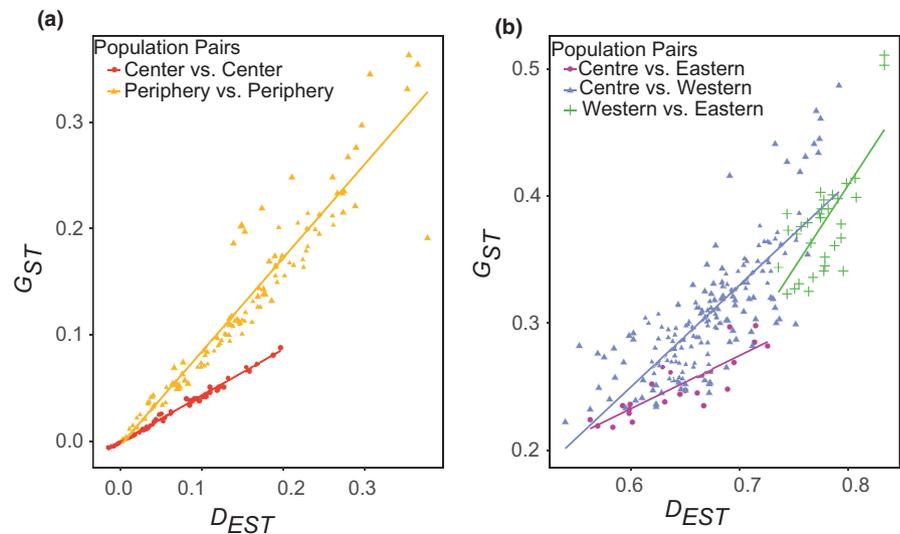
population, the inferred effective population size (N_A) was very low 402 (95% CI: 91–4,740). The relative median of the absolute errors (RMAE) were generally low ranging from 0.19 for the effective population size of the Southern East Italian sub-cluster to 0.25 for the effective population size of South Alboran sub-cluster. Higher value was observed for the ancestral population with RMAE equal to 0.40 for N_A. Regarding historical parameters, the first divergence time between the ancestral pool and the Southern East Italian sub-cluster (t_0; see Figure 2) was 40,400 generations (95% CI: 16,300–49,300) overlapping with the second event (t_1 = 22,100 generations [95% CI: 8,560–38,200]). The remaining divergent events took place between 4,580 (95% CI: 1,220–7,770) and 1,300 (95% CI: 242–5,270) generations ago for t_2 and t_3, respectively. Associated RMAE values ranged from 0.190 for t_0 to 0.350 for t_3. All the results are shown in Table 2.

MIGRAINE analyses confirmed the relatively low effective population sizes suggested by the ABC analyses, with θ_{cur} ranging from 0.47 (95% CI: 0.26–0.75) for PM to 4.8 (1.3–35) for DR (Table 4). Considering $\mu = 5*10^{-4}$ (Sun et al., 2012), N ranged from 233 individuals (95% CI: 132–376) for PM to 2,400 individuals (672–17,400) for DR. While the two populations with highest θ_{cur} are DR and ECON from the South Alboran sub-cluster, a geographic trend was observed with higher θ_{cur} estimates in Central compared with Western populations. Twenty-six populations (89%) showed significant past demographic contraction ($N_{ratio} < 1$; see Appendix S5). The interpretation of the Nratio was not as straightforward in the three remaining populations, all from the South Alboran sub-cluster. NREY showed Nratio values that encompass both >1 and <1 (N_{ratio} [95%CI] = 5.6*10^{-4} [1.7*10^{-5} – 7.792]) corresponding to a stable population. DR and ECON showed Nratio >1 (i.e. expanding population). However, in the three populations, the corresponding $2N\mu$ $2N_{anc}\mu$ likelihood surfaces pointed out potential intricate demographic histories (Appendix S5). Focusing on the 26 contracting populations, the point estimates of $T_g\mu$ (the product of the time of occurrence in generation with the mutation rate) ranged between 0.402 (PM) and 2.22 (LAM). These population contractions occurred between 804

(95% CI: 338–1542) and 4,444 (95% CI: 2,494–9,430) generations ago for PM and LAM, respectively. While most of the corresponding 95% CI overlapped, a decreasing trend in $T_g\mu$ point estimates was observed from populations from the Tunisian, the South Eastern Italian and the Spanish and South Alboran sub-clusters (Table 4).

3.4 | Connectivity in Zembra National Park and neighbouring of Cap Bon

The assignment tests indicated that 50 of the 198 individuals (25%) from Zembra and the neighbouring area of Cap Bon were considered as first-generation migrants (FGMs). FGMs were detected in all the 11 sites ranging from three (AIK, ZEM, NHS, MTS) to seven (CAS, LAM). Thirty-two FGMs (64%) could not be assigned to any sites (assignment probability <0.01) and were thus considered as migrants from unsampled sites. The remaining 18 FGMs (36%) were assigned with a probability higher than 0.01 to up to four sites. These putative sources only included five (AAA, AIK, CGD, ZEM and NHS) of the 11 sites. As we allowed for multiple assignments, these sites were identified as putative sources between one (NHS) and 13 (ZEM) times. No FGM was assigned to the six other sites, which included four and two sites from Zembra and Cap Bon, respectively. None of the potential FGMs identified in Zembra were assigned to Cap Bon, but, on the opposite, four of the 11 FGMs identified in Cap Bon were assigned to Zembra.

4 | DISCUSSION

4.1 | Whole distribution range pattern of genetic diversity and structure in *A. calycularis*

Knowledge regarding the spatial pattern of genetic diversity is critical to estimate populations' evolutionary potential and to support conservation planning (Hoban et al., 2020; Laikre et al., 2020).

TABLE 4 MIGRAINE analyses conducted for the 29 populations. Point estimates and 95% CI are shown for the scaled time ($T_g\mu$), the ancestral scaled population size ($\theta_{anc} = 2*N_{anc}*\mu$), the current scaled population size ($\theta_{cur} = 2*N*\mu$) and the corresponding N_{ratio} with μ corresponding to the mutation rate, N_{anc} and N to the ancient and current population size, respectively. All the N_{ratio} are significantly lower than 0 corresponding to a population bottleneck with the exception of DR and ECON (bold), which showed $N_{ratio} > 1$ as expected in expanding populations and NREY (italics), which showed $N_{ratio} = 1$ as expected in a stable population

	$Tg*\mu$ [95% CI]	$2N*\mu$ [95% CI]	$2N_{anc}*\mu$ [95% CI]	Nratio [95% CI]
AAA	2.05 [0.65–3.72]	3.9 [2.76–5.56]	7,089 [26.07–NA]	$5.5*10^{-4}$ [$1.3*10^{-5}$–0.15]
AIK	1.91 [1.22–3.45]	3.37 [2.48–4.56]	19,097 [37.3–NA]	$1.8*10^{-4}$ [$1.2*10^{-5}$–0.09]
CAD	1.84 [1.08–3.15]	3 [2.05–4.47]	105,537 [33.32–NA]	$3*10^{-5}$ [$1.9*10^{-5}$–0.09]
CAS	2.11 [1.25–3.99]	3.88 [2.77–5.37]	122,879 [32.81–NA]	$3*10^{-5}$ [$2.2*10^{-5}$–0.13]
CGD	2.08 [1.23–4.09]	3.96 [2.91–5.36]	16,982 [44.3–NA]	$2.3*10^{-4}$ [$2.6*10^{-5}$–0.067]
TUN	1.83 [0.86–3.6]	3.34 [2.34–4.74]	5,365 [22.24–NA]	$6.2*10^{-4}$ [$1.63*10^{-4}$–0.15]
LAM	2.22 [1.25–4.72]	3.7 [2.55–5.36]	2,833 [33.92–NA]	$1.31*10^{-3}$ [$2.2*10^{-5}$–0.11]
ZEM	2.09 [0.88–3.21]	3.71 [2.84–4.82]	15,233 [31.27–NA]	$2.4*10^{-4}$ [$1.87*10^{-4}$–0.12]
BBE	1.44 [0.5–2.76]	2.43 [1.69–3.44]	2031 [19.26–NA]	$1.19*10^{-3}$ [$5.5*10^{-5}$–0.12]
MTS	1.33 [0.77–2.31]	2.42 [1.63–3.58]	27,447 [48.99–NA]	$9*10^{-5}$ [$2.7*10^{-5}$–0.05]
NHS	1.53 [0.68–3.15]	2.56 [1.8–3.65]	60,910 [23.73–NA]	$4*10^{-5}$ [$3*10^{-5}$–0.11]
ALB1	1.09 [0.63–2.01]	1.3 [0.89–1.87]	33,674 [56.73–NA]	$4*10^{-5}$ [$2*10^{-5}$–0.02]
ALB2	1.38 [0.75–2.59]	1.23 [0.84–1.79]	4,932 [18.09–NA]	$2.5*10^{-4}$ [$8*10^{-6}$–0.07]
CATRFO	1.63 [0.9–3.85]	2.22 [1.61–3.05]	47,776 [21.53–NA]	$5*10^{-5}$ [$8*10^{-6}$–0.01]
CL	1.38 [0.76–2.39]	1.46 [1.02–2.04]	31,917 [24.04–NA]	$5*10^{-5}$ [$3.2*10^{-5}$–0.06]
DR	0.07 [0.01–2.03]	4.8 [1.34–34.86]	0.98 [0.46–1.66]	**4.87 [1.89–10.2]**
ECON	0.06 [0–4.17]	4.62 [1.32–55.85]	1.12 [0.51–1.87]	**4.13 [1.41–36.44]**
NI	0.88 [0.52–1.79]	1.26 [0.87–1.81]	28,405 [41.07–NA]	$4*10^{-5}$ [$1.5*10^{-5}$–0.04]
NREY	1.25 [0.01–2.98]	1.34 [0.92–39.97]	2,397 [0.72–81274]	*$5.6*10^{-4}$ [$1.7*10^{-5}$–7.79]*
TH	1.64 [0.92–3.31]	1.62 [1.16–2.26]	10,188 [14.87–NA]	$1.6*10^{-4}$ [$2.7*10^{-5}$–0.08]
ALF	1.42 [0.73–2.91]	1.52 [1.08–2.07]	63,914 [11.24–NA]	$2*10^{-5}$ [$1.7*10^{-5}$–0.06]
ALG	1.31 [0.01–3.08]	1.02 [0.69–1.49]	3,267 [8.19–NA]	$3.1*10^{-4}$ [$1*10^{-5}$–0.44]
ALM	1.33 [0–3.24]	1.32 [0.01–1.87]	35,890 [15.46–NA]	$4*10^{-5}$ [$6*10^{-6}$–0.34]
GAT	0.58 [0.28–1.26]	0.66 [0.39–1.04]	11,230 [33.79–NA]	$6*10^{-5}$ [$1.2*10^{-5}$–0.02]
GRA	1.7 [0.82–3.4]	1.16 [0.77–1.76]	3,534 [13.36–NA]	$3.3*10^{-4}$ [$6.6*10^{-5}$–0.09]
PC	1.87 [0.93–4.33]	1.7 [1.19–2.39]	13,377 [12.35–NA]	$1.3*10^{-4}$ [$2.3*10^{-5}$–0.10]
PM	0.4 [0.19–0.77]	0.47 [0.26–0.75]	11,195 [61.51–NA]	$4*10^{-5}$ [$1*10^{-5}$–0.01]
PAL	1.79 [0.93–4]	2.53 [1.89–3.37]	23,613 [40.48–NA]	$1.1*10^{-4}$ [$3.2*10^{-5}$–0.06]
PAN	1.95 [1.08–4.43]	2.38 [1.73–3.29]	34,525 [13.79–NA]	$7*10^{-5}$ [$1.8*10^{-5}$–0.17]

Here, considering two different measures of geographic peripherality, we demonstrated significant decreases in genetic diversity (H_e and $Ar_{(10)}$) combined with a significant increase in genetic isolation (population-specific F_{ST}s) and nearness to fixation (G_{ST}s vs. DESTs) from the Centre to the Eastern periphery and from the Centre to the Western periphery in *A. calycularis*. The genetic diversity is thus highly heterogeneously distributed across the distribution range of *A. calycularis* with a strong pattern of structure.

The clustering analyses revealed low level of admixture among highly differentiated genetic clusters. In line with this result and supporting the heterogeneous distribution of genetic diversity, the lower value of the global G_{ST} (nearness to fixation; Jost et al., 2018) compared with the D_{EST} (allelic differentiation; Jost et al., 2018) suggests that some alleles are unshared across the range distribution

(Jost et al., 2018). The linear regressions between pairwise D_{EST}s and G_{ST}s complement this result. In the first set of analyses (i.e. $-0.1 < D_{EST}$s < 0.4), a steeper linear regression was observed among population pairs from the same Periphery (i.e. within the Western or Eastern Periphery) compared with population pairs from the Centre of the distribution range. For the same D_{EST}, the corresponding G_{ST} is higher in peripheral populations, which are thus closer to fixation, compared with central populations. In the second set of analyses (i.e. $0.55 < D_{EST}$s < 0.85), the linear regression between D_{EST} and G_{ST} is steeper for Centre versus Western Periphery populations compared with Centre versus Eastern periphery populations, suggesting a higher genetic differentiation of the Western periphery. The population-specific F_{ST}s corroborated the relative genetic isolation of the peripheral populations with the highest values observed across the Western

Periphery. Interestingly, nine of the ten highest pairwise D_{EST}s (>0.79) involved one population from the Western Periphery and one population from the Eastern Periphery highlighting the totally different genetic pools of the populations located at the two peripheries.

Centre to peripheries negative genetic gradients were reported in different species (Eckert et al., 2008; Pironon et al., 2017) including corals (e.g. Andras et al., 2013; Miller & Ayre, 2004; Nunes et al., 2009). Focusing on the Mediterranean Sea, recent studies also reported regional negative genetic gradients (Boscari et al., 2019; Ledoux et al., 2018). Our work goes one step further as most of these studies focused on one particular area of the distribution range (Eckert et al., 2008; Guo, 2012). Indeed, considering most of the species distribution range, we demonstrate the occurrence of multidirectional (eastward and westward) longitudinal genetic gradients, involving different alleles, and going along with a stronger genetic differentiation and isolation of the peripheral populations. Whether or not this pattern will be retained after adding Algerian populations, which are situated in close proximity to the hypothetical geographic Centre of the current distribution range, is an open question. Unfortunately, these populations remain challenging to sample. However, it is noteworthy the genetic gradients are supported considering two different measures (DC and DNRL) capturing different aspects of peripherality (see Methods). The coefficients of determination of the linear models based on DNRL were similar (population-specific F_{ST}) or higher (H_e and $Ar_{(10)}$) than those based on DC. We thus assume these genetic patterns should not be disrupted by adding Algerian populations. However, their genotyping and the genotyping of atypical populations (e.g. Adriatic Sea; Central Italy) are needed to further characterize the genetic variation in *A. calycularis*.

4.2 | "Postglacial range expansion hypothesis" versus "Central–peripheral hypothesis": insights into the underlying processes

Disentangling the relative influence of historical (i.e. postglacial sequential recolonization) versus contemporary (i.e. low effective population size, demographic isolation) processes on neutral genetic diversity gradient is a challenging task (Eckert et al., 2008; but see Johansson et al., 2006). Under the postglacial range expansion hypothesis, negative gradients result from a sequential recolonization involving serial founder events. We thus expect the Centre populations to be founded earlier than the Periphery populations; hence, those peripheral populations should show stronger genetic imprints of founder events. On the other hand, the central–peripheral hypothesis relies on a low effective population size and thus higher demo-genetic stochasticity in peripheral compared with central populations due for instance to less optimal environmental conditions in peripheral habitats.

The approximate Bayesian computations combined with the maximum-likelihood analyses in MIGRAINE give support to the postglacial range expansion hypothesis, suggesting an intricate evolutionary history in *A. calycularis*. The most likely evolutionary scenario

(Scenario 5) involved a sequential foundation for the four different sub-clusters. In this scenario, a first divergence event from the ancestral pool led to the Southern East Italian sub-cluster, potentially concomitant with the divergence of the Tunisian sub-cluster, and followed by the divergences of the Spanish and the South Alboran sub-clusters. While the RMAE associated with the estimated parameters call for cautious interpretation, it is noteworthy the divergence events are widely distributed in time, ranging from 40,400 (95% CI: 16,300–49,300) to 1,300 (95%CI: 242–5,270) generations ago. The generation time in *A. calycularis* is unknown. However, the three- to five-year-olds for sexual maturity observed in the related species *Leptopsammia pruvoti* (Goffredo et al., 2006) place the sub-cluster divergences on the two sides of the Last Glacial Maximum (24–18,000 years ago), with the divergence of the Southern East Italian sub-cluster 121,000 to 202,000 years ago and the divergence between the Spanish and South Alboran sub-clusters only 3,900 to 6,500 years ago. Refining these results, the maximum-likelihood approach also supports the occurrence of a sequence of demographic events at the population scale. All the populations but ECON, DR and NREY showed a demographic contraction shared among the last 804 to 4,444 generations (setting $\mu = 5*10^{-4}$). The oldest contractions are observed in the Central and the Southern East Italian sub-clusters, while the most recent ones are observed in the Spanish and South Alboran sub-clusters. Focusing on point estimates and considering three- and five-year generation time, these events happened between 22,220 and 4,020 and 13,333 and 2,412 years ago, respectively. This temporal framework is thus consistent with a potential impact of the LGM. In the meantime, the maximum-likelihood approach revealed the higher current scaled effective population sizes (θ_{cur}) in the Centre populations (e.g. CGD = 3.96 [2.91–5.36]) compared with Western populations (e.g. GAT = 0.66 [0.39–1.04]). This trend, which is only challenged by the two expanding populations from the South Alboran sub-clusters (ECON, DR), is expected in the central–peripheral hypothesis. Accordingly, we suggest the postglacial range expansion to be a major driver of the current negative genetic gradients yet the central-peripheral hypothesis can not be totally ruled out. As mentioned previously, Algerian samples should be considered to refine this result. Keeping in mind the sea-level variations during the Last Glacial Maximum, it is unlikely that the location of the ancestral population overlapped the current centre of distribution range. However, we expect the Algerian populations to be closer to the ancestral populations than the populations from the Periphery and, accordingly, to be founded before or simultaneously with the Tunisian populations. Moreover, we call for complementary demographic studies (e.g. Ocaña et al., 2009; Goffredo et al., 2006; Prada et al., 2019) to formally characterize the impact of contemporary demo-genetic stochasticity on the pattern of genetic diversity (see Johansson et al., 2006).

An imprint of postglacial sequential recolonization on the contemporary pattern of genetic diversity was previously reported in the Mediterranean red gorgonian, *Paramuricea clavata* (Ledoux et al., 2018), and suspected in another coral, *Leptosammia pruvoti*, in the Adriatic Sea (Boscari et al., 2019). In spite of their relatively contrasted ecology (e.g. habitat, distribution range), these three

species seem to show comparable genetic imprints of past climatic fluctuations. Similar legacy of postglacial recolonization processes is widely acknowledged in terrestrial species (e.g. Hewitt, 2000) and is expected in low dispersal marine species (Hellberg et al., 2002). Whether this trend can be generalized to other low dispersal Mediterranean habitat-forming species thus deserves further attention, owing to its conservation implications.

4.3 | General conservation implications and functioning of the Zembra National Park, a hotspot of genetic diversity

The need to account for genetic diversity is widely acknowledged by conservation biologists, yet it remains barely considered by policymakers (Hoban et al., 2020; Laikre et al., 2020). One of the main outputs of our study, supported by the approximate Bayesian computations and the maximum-likelihood approach, is the relatively low effective population sizes in *A. calycularis*. Considering $\mu = 5*10^{-4}$, most of the population size estimates are lower than 3,000 individuals with various populations (e.g. PM, GAT and ALG) showing values close to 500 individuals, the limit to consider a population as "genetically safe" (Jamieson & Allendorf, 2012). Included in Annex II of the CITES, *A. calycularis* is considered as "vulnerable" under Bern and Barcelona conventions and of "Least Concerned" in Mediterranean regional IUCN red list due to its demographic stability (Otero et al., 2017). Nevertheless, the low effective population sizes revealed here deserve further attention from policymakers and should be used to complement the conservation status of the species. Indeed, these low effective population sizes question the adaptive potential of the species in the current disturbance regime. Besides, the occurrence of well-defined genetic clusters with contrasted evolutionary histories, including potentially deep divergences and highly restricted gene flow, supports the definition of different management units covering the species distribution range. We suggest these units to overlap the four genetic sub-clusters, but complementary sampling (e.g. Algerian and Adriatic regions) and characterization of the pattern of adaptive diversity should refine this strategy. Combining this pattern with the estimates of effective population sizes should allow to further guide conservation actions as exemplified here for two contrasted cases: the Spanish and the Tunisian sub-clusters.

The Spanish sub-cluster is almost exclusively composed by populations with effective population sizes below the "genetically safe" limit of 500 individuals. This may be expected considering the relatively recent foundation of this sub-cluster. Nevertheless, these populations may harbour limited potential for adaptation in the current environmental context. Teixidó et al. (2020) recently suggested potential for local adaptation in an atypical population at the Eastern Periphery. Estimating the genetic parameters in this particular population may give first insights into the interaction between effective population size and adaptive capacities in *A. calycularis*. Meanwhile, the populations from the Spanish sub-cluster should be targeted by

dedicated conservation plans to restrain, for instance, the impact of local stressors.

The Tunisian sub-cluster, which includes the Zembra National Park, encompasses most of the populations with high effective population sizes. Boudouresque et al. (1986) were the first to point out that *A. calycularis* was particularly abundant in the Park. We complement this seminal study characterizing the processes underlying this hotspot of genetic diversity. The IBD revealed among the populations from Tunisian sub-cluster is characterized by a neighbourhood size (Nb = 91 individuals) similar to published values for other Mediterranean corals (e.g. Nb = 55 individuals for *P. clavata*; Ledoux et al., 2018), supporting a spatially limited dispersal with low population sizes. Considering the lack of genetic differentiation among populations separated by up to 4.75 km, gene flow among populations is likely to occur within the Zembra National Park (3.69 km^2). The assignment analyses showed that these populations are characterized by contrasted roles with regard to the connectivity of the system. The connectivity between Zembra and Cap Bon areas seems highly asymmetric. All the first-generation migrants (FGMs) shared between the two areas were found in Cap Bon and sourced in Zembra, suggesting spillover from the National Park towards the neighbouring area. This unidirectional pattern was expected considering the regional oceanographic features, and more particularly, the eastward Atlantic Tunisian Current (Sorgente et al., 2011). FGMs were identified in all the 11 Tunisian populations, but they only come from five populations. Those five source populations, and particularly ZEM and CDS, which were identified as potential sources in more than 70% of the cases, require specific conservation attention. A related point to consider here is the lack of assignment for 64% of the FGMs. The Zembra National Park is thus connected to some degree with unsampled area(s), likely on the western Tunisian coast considering the local oceanographic features (Sorgente et al., 2011). While it is important to concentrate management efforts on Zembra, the status of this hotspot of diversity seems unambiguously linked to neighbouring unprotected populations, reinforcing the relevance to enforce the protection at the species level.

5 | CONCLUSION

In the warming Mediterranean Sea (Bensoussan et al., 2019; Cramer et al., 2018), the evolution of marine biodiversity is a matter of concern (Garrabou et al., 2009, 2021). Shifts in species distribution ranges are expected with "losers and winners" and potential consequences at the community level (Gómez-Gras et al., 2019, 2021). To date, most of the efforts in this topic focused on species negatively impacted by climate change (e.g. Arizmendi-Mejía, Ledoux, et al., 2015; Crisci et al., 2017; Ledoux et al., 2015; Torrents et al., 2008). *Astroides calycularis* may offer a complementary perspective. First, it is considered as a warm-water species, which may potentially benefit from the sea temperature increase expanding its distribution range (Bianchi, 2007; Kružić et al., 2002; but see Movilla et al., 2016). Then, addressing the impact of warming on biodiversity through the lens of peripheral

populations is widely acknowledged (e.g. Hampe & Petit, 2005; Sexton et al., 2009). Accordingly, we identified in this study natural experimental setups where to concentrate efforts to decipher "peripheral population-by-warming environment" interactions. Overall, these results combined with previous study (Casado-Amezúa et al., 2012; Teixidó et al., 2020) stand *A. calycularis* as a highly relevant model to study the evolution of Mediterranean marine diversity facing warming.

CONFLICT OF INTEREST
None declared.

PEER REVIEW
The peer review history for this article is available at https://publons.com/publon/10.1111/ddi.13382.

DATA AVAILABILITY STATEMENT
Microsatellite genotypes are available on Dryad (DOI https://doi.org/10.5061/dryad.xgxd254gw).

ORCID
Jean-Baptiste Ledoux 🄳 https://orcid.org/0000-0001-8796-6163

REFERENCES

Andras, J. P., Rypien, K. L., & Harvell, C. D. (2013). Range-wide population genetic structure of the Caribbean sea fan coral, *Gorgonia ventalina*. *Molecular Ecology*, *22*, 56–73. https://doi.org/10.1111/mec.12104

Arizmendi-Mejía, R., Ledoux, J.-B., Civit, S., Antunes, A., Thanopoulou, Z., Garrabou, J., & Linares, C. (2015). Demographic responses to warming: Reproductive maturity and sex influence vulnerability in an octocoral. *Coral Reefs*, *34*, 1207–1216. https://doi.org/10.1007/s00338-015-1332-9

Arizmendi-Mejía, R., Linares, C., Garrabou, J., Antunes, A., Ballesteros, E., Cebrian, E., Díaz, D., & Ledoux, J.-B. (2015). Combining genetic and demographic data for the conservation of a Mediterranean marine habitat-forming species. *PLoS One*, *10*, e0119585. https://doi.org/10.1371/journal.pone.0119585

Aurelle, D., Ledoux, J.-B., Rocher, C., Borsa, P., Chenuil, A., & Féral, J.-P. (2011). Phylogeography of the red coral (*Corallium rubrum*): Inferences on the evolutionary history of a temperate gorgonian. *Genetica*, *139*, 855–869. https://doi.org/10.1007/s10709-011-9589-6

Austerlitz, F., Jung-Muller, B., Godelle, B., & Gouyon, P.-H. (1997). Evolution of coalescence times, genetic diversity and structure during colonization. *Theoretical Population Biology*, *51*, 148–164. https://doi.org/10.1006/tpbi.1997.1302

Austerlitz, F., Mariette, S., Machon, N., Gouyon, P. H., & Godelle, B. (2000). Effects of colonization processes on genetic diversity: Differences between annual plants and tree species. *Genetics*, *154*, 1309–1321. https://doi.org/10.1093/genetics/154.3.1309

Belkhir, K., Borsa, P., Chikhi, L., Raufaste, N., & Bonhomme, F. (2004). *GENETIX 4.05, Logiciel Sous Windows TM Pour La Génétique Des Populations*.

Benjamini, Y., & Hochberg, Y. (1995). Controlling the false discovery rate – A practical and powerful approach to multiple testing. *Journal of the Royal Statistical Society: Series B (Methodological)*, *57*, 289–300. https://doi.org/10.1111/j.2517-6161.1995.tb02031.x

Bensoussan, N., Cebrian, E., Dominici, J. M., Kersting, D. K., Kipson, S., Kizilkaya, Z., Ocana, O., Peirache, M., Zuberer, F., Ledoux, J. B., Linares, C., Zabala, M., Buongiorno Nardelli, B., Pisano, A., & Garrabou, J. (2019). Using CMEMS and the Mediterranean Marine protected Area sentinel network to track ocean warming effects in coastal areas. In: Copernicus Marine Service Ocean State Report, Issue 3. *Journal of Operational Oceanography*, *12*, 65–73. https://doi.org/10.1080/1755876X.2019.1633075

Bianchi, C. N. (2007). Biodiversity issues for the forthcoming tropical Mediterranean Sea. *Hydrobiologia*, *580*, 7–21. https://doi.org/10.1007/s10750-006-0469-5

Boscari, E., Abbiati, M., Badalamenti, F., Bavestrello, G., Benedetti-Cecchi, L. et al. (2019). A population genomics insight by 2b-RAD reveals populations' uniqueness along the Italian coastline in *Leptopsammia pruvoti* (Scleractinia, Dendrophylliidae), (A. Zhan, Ed.). *Diversity and Distributions*, *25*, 1101–1117. https://doi.org/10.1111/ddi.12918

Boudouresque, C.-F., Harmelin, J.-G., & Jeudy de Grissac, A. (1986). *Le benthos marin de l'île de Zembra (Parc national, Tunisie)*. Marseille.

Cahill, A. E., De Jode, A., Dubois, S., Bouzaza, Z., Aurelle, D., Boissin, E., Chabrol, O., David, R., Egea, E., Ledoux, J.-B., Mérigot, B., Weber, A.-T., & Chenuil, A. (2017). A multispecies approach reveals hot spots and cold spots of diversity and connectivity in invertebrate species with contrasting dispersal modes. *Molecular Ecology*, *26*, 6563–6577. https://doi.org/10.1111/mec.14389

Casado-Amezúa, P., Goffredo, S., Templado, J., & Machordom, A. (2012). Genetic assessment of population structure and connectivity in the threatened Mediterranean coral *Astroides calycularis* (Scleractinia, Dendrophylliidae) at different spatial scales. *Molecular Ecology*, *21*, 3671–3685. https://doi.org/10.1111/j.1365-294X.2012.05655.x

Chapuis, M.-P., & Estoup, A. (2007). Microsatellite null alleles and estimation of population differentiation. *Molecular Biology and Evolution*, *24*, 621–631. https://doi.org/10.1093/molbev/msl191

Cornuet, J.-M., Pudlo, P., Veyssier, J., Dehne-Garcia, A., Gautier, M., Leblois, R., … Estoup, A. (2014). DIYABC v2.0: A software to make approximate Bayesian computation inferences about population history using single nucleotide polymorphism, DNA sequence and microsatellite data. *Bioinformatics*, *30*, 1187–1189. https://doi.org/10.1093/bioinformatics/btt763

Cornuet, J.-M., Ravigné, V., & Estoup, A. (2010). Inference on population history and model checking using DNA sequence and microsatellite

data with the software DIYABC (v1.0). *BMC Bioinformatics*, 11, 401. https://doi.org/10.1186/1471-2105-11-401

Cramer, W., Guiot, J., Fader, M., Garrabou, J., Gattuso, J.-P., Iglesias, A., Lange, M. A., Lionello, P., Llasat, M. C., Paz, S., Peñuelas, J., Snoussi, M., Toreti, A., Tsimplis, M. N., & Xoplaki, E. (2018). Climate change and interconnected risks to sustainable development in the Mediterranean. *Nature Climate Change*, 8, 972–980. https://doi.org/10.1038/s41558-018-0299-2

Crisci, C., Ledoux, J.-B., Mokhtar- Jamaï, K., Bally, M., Bensoussan, N., Aurelle, D., Cebrian, E., Coma, R., Féral, J.-P., La Rivière, M., Linares, C., López-Sendino, P., Marschal, C., Ribes, M., Teixidó, N., Zuberer, F., & Garrabou, J. (2017). Regional and local environmental conditions do not shape the response to warming of a marine habitat-forming species. *Scientific Reports*, 7, 5069. https://doi.org/10.1038/s41598-017-05220-4

Dalongeville, A., Andrello, M., Mouillot, D., Lobreaux, S., Fortin, M.-J., Lasram, F., Belmaker, J., Rocklin, D., & Manel, S. (2018). Geographic isolation and larval dispersal shape seascape genetic patterns differently according to spatial scale. *Evolutionary Applications*, 11, 1437–1447. https://doi.org/10.1111/eva.12638

de Iorio, M., & Griffiths, R. C. (2004a). Importance sampling on coalescent histories. *Advances in Applied Probability*, 36, 417–433.

de Iorio, M., & Griffiths, R. C. (2004b). Importance sampling on coalescent histories. II. Subdivided population models. *Advances in Applied Probability*, 36, 434–454. https://doi.org/10.1017/S0001867800013550

Eckert, C. G., Samis, K. E., & Lougheed, S. C. (2008). Genetic variation across species' geographical ranges: The central-marginal hypothesis and beyond. *Molecular Ecology*, 17, 1170–1188. https://doi.org/10.1111/j.1365-294X.2007.03659.x

Evanno, G., Regnaut, S., & Goudet, J. (2005). Detecting the number of clusters of individuals using the software STRUCTURE: A simulation study. *Molecular Ecology*, 14, 2611–2620. https://doi.org/10.1111/j.1365-294X.2005.02553.x

Fisher, R. A. (1930). *The genetical theory of natural selection*. Clarendon Press.

Foll, M., & Gaggiotti, O. E. (2006). Identifying the environmental factors that determine the genetic structure of Populations. *Genetics*, 174, 875–891. https://doi.org/10.1534/genetics.106.059451

Frankham, R. (1995). Conservation genetics. *Annual Review of Genetics*, 29, 305–327. https://doi.org/10.1146/annurev.ge.29.120195.001513

Gaggiotti, O. E., & Foll, M. (2010). Quantifying population structure using the F-model. *Molecular Ecology Resources*, 10, 821–830. https://doi.org/10.1111/j.1755-0998.2010.02873.x

Garrabou, J., Coma, R., Bensoussan, N., Bally, M., Chevaldonné, P., Cigliano, M., Diaz, D., Harmelin, J. G., Gambi, M. C., Kersting, D. K., Ledoux, J. B., Lejeusne, C., Linares, C., Marschal, C., Pérez, T., Ribes, M., Romano, J. C., Serrano, E., Teixido, N., ... Cerrano, C. (2009). Mass mortality in Northwestern Mediterranean rocky benthic communities: Effects of the 2003 heat wave. *Global Change Biology*, 15, 1090–1103. https://doi.org/10.1111/j.1365-2486.2008.01823.x

Garrabou, J., Ledoux, J. B., Bensoussan, N., Gómez-Gras, D., & Linares, C. (2021). Sliding Toward the Collapse of Mediterranean Coastal Marine Rocky Ecosystems. In J. G. Canadell, & R. B. Jackson (eds), *Ecosystem Collapse and Climate Change. Ecological Studies (Analysis and Synthesis)* (Vol, 241). Springer. https://doi.org/10.1007/978-3-030-71330-0_11

Gazulla, C. R., López-Sendino, P., Antunes, A., Aurelle, D., Montero-Serra, I., Dominici, J.-M., Linares, C., Garrabou, J., & Ledoux, J.-B. (2021). Demo-genetic approach for the conservation and restoration of a habitat forming Octocoral: The Case of Red Coral, Corallium rubrum, in the Réserve Naturelle de Scandola. *Frontiers in Marine Science*, 8, 633057. https://doi.org/10.3389/fmars.2021.633057

Ghanem, R., Ben Souissi, J., Ledoux, J., Linares, C., & Garrabou, J. (2021). Population structure and conservation status of the white gorgonian *Eunicella singularis* (Esper, 1791) in Tunisian waters (Central Mediterranean). *Mediterranean Marine Science*, 22(2), 362–371. https://doi.org/10.12681/mms.24984

Ghanem, R., Soufi-Kechaou, E., Ben, S. J., Linares, C., Ledoux, J. B., & Garrabou, J. (2019). Demography and disturbance levels of the coral *Astroides calycularis* (Pallas, 1766) in the Tunisian Marine Protected Area of Zembra (Central Mediterranean). In H. Langar, & A. Ouerghi (Eds.), *UNEP/MAP – SPA/RAC, 2019* (pp. 52–56). Proceedings of the 3rd Mediterranean Symposium on the conservation of Coralligenous & other Calcareous Bio-Concretions (Antalya, Turkey, 15–16 January 2019). SPA/RAC Publications, 135 p.

Goffredo, S., Airi, V., Radetić, J., & Zaccanti, F. (2006). Sexual reproduction of the solitary sunset cup coral Leptopsammia pruvoti (Scleractinia, Dendrophylliidae) in the Mediterranean. 2. Quantitative aspects of the annual reproductive cycle. *Marine Biology*, 148, 923–931. https://doi.org/10.1007/s00227-005-0137-8

Goffredo, S., Gasparini, G., Marconi, G., Puntignano, M. T., Pazzini, C., & Zaccanti, F. (2010). Gonochorism and planula brooding in the Mediterranean endemic orange coral *Astroides calycularis* (Scleractinia: Dendrophylliidae): Morphological aspects of gametogenesis and ontogenesis. *Marine Biology Research*, 10, 421–436.

Gómez-Gras, D., Linares, C., de Caralt, S., Cebrian, E., Frleta-Valić, M., Montero-Serra, I., Pagès-Escolà, M., López-Sendino, P., & Garrabou, J. (2019). Response diversity in Mediterranean coralligenous assemblages facing climate change: Insights from a multispecific thermo-tolerance experiment. *Ecology and Evolution*, 9, 4168–4180. https://doi.org/10.1002/ece3.5045

Gómez-Gras, D., Linares, C., Dornelas, M., Madin, J. S., Brambilla, V., Ledoux, J.-B., López-Sendino, P., Bensoussan, N., & Garrabou, J. (2021). Climate change transforms the functional identity of Mediterranean coralligenous assemblages. *Ecology Letters*, 24, 1038–1051. https://doi.org/10.1111/ele.13718

Grubelić, I., Antolić, B., Despalatović, M., Grbec, B., & Paklar, G. B. (2004). Effect of climatic fluctuations on the distribution of warm-water coral *Astroides calycularis* in the Adriatic Sea: New records and review. *Journal of the Marine Biological Association of the UK*, 84, 599–602. https://doi.org/10.1017/S0025315404009609h

Guo, Q. (2012). Incorporating latitudinal and central-marginal trends in assessing genetic variation across species ranges. *Molecular Ecology*, 21, 5396–5403. https://doi.org/10.1111/mec.12012

Hampe, A., & Petit, R. J. (2005). Conserving biodiversity under climate change: The rear edge matters. *Ecology Letters*, 8, 461–467. https://doi.org/10.1111/j.1461-0248.2005.00739.x

Hardie, D. C., & Hutchings, J. A. (2010). Evolutionary ecology at the extremes of species' ranges. *Environmental Reviews*, 18, 1–20. https://doi.org/10.1139/A09-014

Hellberg, M. E., Burton, R. S., Neigel, J. E., & Palumbi, S. R. (2002). Genetic assessment of connectivity among marine populations. *Bulletin of Marine Science*, 70(1), 273–290.

Hewitt, G. (2000). The genetic legacy of the Quaternary ice ages. *Nature*, 405, 907–913. https://doi.org/10.1038/35016000

Hoban, S., Bruford, M., D'Urban Jackson, J., Lopes-Fernandes, M., Heuertz, M., Hohenlohe, P. A., Paz-Vinas, I., Sjögren-Gulve, P., Segelbacher, G., Vernesi, C., Aitken, S., Bertola, L. D., Bloomer, P., Breed, M., Rodríguez-Correa, H., Funk, W. C., Grueber, C. E., Hunter, M. E., Jaffe, R., ... Laikre, L. (2020). Genetic diversity targets and indicators in the CBD post-2020 Global Biodiversity Framework must be improved. *Biological Conservation*, 248, 108654. https://doi.org/10.1016/j.biocon.2020.108654

Hughes, A. R., Inouye, B. D., Johnson, M. T. J., Underwood, N., & Vellend, M. (2008). Ecological consequences of genetic diversity. *Ecology Letters*, 11, 609–623. https://doi.org/10.1111/j.1461-0248.2008.01179.x

Jamieson, I. G., & Allendorf, F. W. (2012). How does the 50/500 rule apply to MVPs? *Trends in Ecology & Evolution*, 27(10), 578–584. https://doi.org/10.1016/j.tree.2012.07.001

Johansson, M., Primmer, C. R., & Merilä, J. (2006). History vs. current demography: Explaining the genetic population structure of the common frog (*Rana temporaria*). *Molecular Ecology*, 15, 975–983. https://doi.org/10.1111/j.1365-294X.2006.02866.x

Jombart, T. (2008). adegenet: A R package for the multivariate analysis of genetic markers. *Bioinformatics*, 24, 1403–1405. https://doi.org/10.1093/bioinformatics/btn129

Jombart, T., Devillard, S., & Balloux, F. (2010). Discriminant analysis of principal components: A new method for the analysis of genetically structured populations. *BMC Genetics*, 11, 94. https://doi.org/10.1186/1471-2156-11-94

Jost, L. (2008). GST and its relatives do not measure differentiation. *Molecular Ecology*, 17, 4015–4026. https://doi.org/10.1111/j.1365-294X.2008.03887.x

Jost, L., Archer, F., Flanagan, S., Gaggiotti, O., Hoban, S., & Latch, E. (2018). Differentiation measures for conservation genetics. *Evolutionary Applications*, 11, 1139–1148. https://doi.org/10.1111/eva.12590

Kokko, H., Chaturvedi, A., Croll, D., Fischer, M. C., Guillaume, F., Karrenberg, S., Kerr, B., Rolshausen, G., & Stapley, J. (2017). Can evolution supply what ecology demands?. *Trends in Ecology & Evolution*, 32, 187–197. https://doi.org/10.1016/J.TREE.2016.12.005

Kružić, P., Zibrowius, H., & Pozar-Domac, A. (2002). Actiniaria and Scleractinia (Cnidaria, Anthozoa) from the Adriatic Sea (Croatia): First records, confirmed occurrences and significant range extensions of certain species. *The Italian Journal of Zoology*, 69, 345–353. https://doi.org/10.1080/11250000209356480

Laikre, L., Hoban, S., Bruford, M. W., Segelbacher, G., Allendorf, F. W., Gajardo, G., Rodríguez, A. G., Hedrick, P. W., Heuertz, M., Hohenlohe, P. A., Jaffé, R., Johannesson, K., Liggins, L., MacDonald, A. J., OrozcoterWengel, P., Reusch, T. B. H., Rodríguez-Correa, H., Russo, I.-R., Ryman, N., & Vernesi, C. (2020). Post-2020 goals overlook genetic diversity. *Science*, 367, 1083–1085. https://doi.org/10.1126/science.abb2748

Lambeck, K., & Purcell, A. (2005). Sea-level change in the Mediterranean Sea since the LGM: Model predictions for tectonically stable areas. *Quaternary Science Reviews*, 24, 1969–1988. https://doi.org/10.1016/j.quascirev.2004.06.025

Leblois, R., Pudlo, P., Néron, J., Bertaux, F., Reddy Beeravolu, C., Vitalis, R., & Rousset, F. (2014). Maximum-likelihood inference of population size contractions from microsatellite data. *Molecular Biology and Evolution*, 31, 2805–2823. https://doi.org/10.1093/molbev/msu212

Ledoux, J.-B., Aurelle, D., Bensoussan, N., Marschal, C., Féral, J.-P., & Garrabou, J. (2015). Potential for adaptive evolution at species range margins: Contrasting interactions between red coral populations and their environment in a changing ocean. *Ecology and Evolution*, 5, 1178–1192. https://doi.org/10.1002/ece3.1324

Ledoux, J.-B., Frleta-Valić, M., Kipson, S., Antunes, A., Cebrian, E., Linares, C., Sánchez, P., Leblois, R., & Garrabou, J. (2018). Postglacial range expansion shaped the spatial genetic structure in a marine habitat-forming species: Implications for conservation plans in the Eastern Adriatic Sea. *Journal of Biogeography*, 45, 2645–2657. https://doi.org/10.1111/jbi.13461

Ledoux, J.-B., Frias-Vidal, S., Montero-Serra, I., Antunes, A., Casado Bueno, C., Civit, S., Lopez-Sendino, P., Linares, C., & Garrabou, J. (2020). Assessing the impact of population decline on mating system in the overexploited Mediterranean red coral. *Aquatic Conservation: Marine and Freshwater Ecosystems*, 30, 1149–1159. https://doi.org/10.1002/aqc.3327

Ledoux, J.-B., Mokhtar-Jamaï, K., Roby, C., Féral, J.-P., Garrabou, J., & Aurelle, D. (2010). Genetic survey of shallow populations of the Mediterranean red coral [*Corallium rubrum* (Linnaeus, 1758)]: New insights into evolutionary processes shaping nuclear diversity and implications for conservation. *Molecular Ecology*, 19, 675–690. https://doi.org/10.1111/j.1365-294X.2009.04516.x

Lukoschek, V., Riginos, C., & van Oppen, M. J. H. (2016). Congruent patterns of connectivity can inform management for broadcast spawning corals on the Great Barrier Reef. *Molecular Ecology*, 25, 3065–3080. https://doi.org/10.1111/mec.13649

Magris, R. A., Andrello, M., Pressey, R. L., Mouillot, D., Dalongeville, A., Jacobi, M. N., & Manel, S. (2018). Biologically representative and well-connected marine reserves enhance biodiversity persistence in conservation planning. *Conservation Letters*, 11(4), e12439. https://doi.org/10.1111/conl.12439

Manel, S., Loiseau, N., Andrello, M., Fietz, K., Goñi, R., Forcada, A., Lenfant, P., Kininmonth, S., Marcos, C., Marques, V., Mallol, S., Pérez-Ruzafa, A., Breusing, C., Puebla, O., & Mouillot, D. (2019). Long-distance benefits of marine reserves: Myth or reality?. *Trends in Ecology & Evolution*, 34, 342–354. https://doi.org/10.1016/j.tree.2019.01.002

Meirmans, P. G., & vanTienderen, P. H. (2004). GENOTYPE and GENODIVE: Two programs for the analysis of genetic diversity of asexual organisms. *Molecular Ecology Notes*, 4, 792–794. https://doi.org/10.1111/j.1471-8286.2004.00770.x

Merino-Serrais, P., Casado-Amezúa, P., Ocaña, Ó., Templado, J., & Machordom, A. (2012). Slight genetic differentiation between western and eastern limits of *Astroides calycularis* (Pallas, 1776) (Anthozoa, Scleractinia, Dendrophylliidae) distribution inferred from COI and ITS sequences. *Graellsia*, 68, 207–218.

Miller, K. J., & Ayre, D. J. (2004). The role of sexual and asexual reproduction in structuring high latitude populations of the reef coral *Pocillopora damicornis*. *Heredity (Edinburgh)*, 92, 557–568. https://doi.org/10.1038/sj.hdy.6800459

Mouillot, D., Albouy, C., Guilhaumon, F., Ben Rais Lasram, F., Coll, M., Devictor, V., Meynard, C. N., Pauly, D., Tomasini, J. A., Troussellier, M., Velez, L., Watson, R., Douzery, E. J. P., & Mouquet, N. (2011). Protected and threatened components of fish biodiversity in the Mediterranean sea. *Current Biology*, 21, 1044–1050. https://doi.org/10.1016/j.cub.2011.05.005

Movilla, J., Calvo, E., Coma, R., Serrano, E., López-Sanz, À., & Pelejero, C. (2016). Annual response of two Mediterranean azooxanthellate temperate corals to low-pH and high-temperature conditions. *Marine Biology*, 163, 135. https://doi.org/10.1007/s00227-016-2908-9

Nei, M. (1973). Analysis of gene diversity in subdivided populations. *Proceedings of the National Academy of Sciences of the United States of America*, 70, 3321–3323. https://doi.org/10.1073/pnas.70.12.3321

Nei, M. (1987). *Molecular evolutionary genetics*. Columbia University Press.

Nunes, F., Norris, R. D., & Knowlton, N. (2009). Implications of isolation and low genetic diversity in peripheral populations of an amphi-Atlantic coral. *Molecular Ecology*, 18, 4283–4297. https://doi.org/10.1111/j.1365-294X.2009.04347.x

Ocaña, O. (2012). *Estudio y ordenación de los bancos de Astroides calycularis para la mejor gestión de los espacios protegidos por la red natura (LIC) en Ceuta y Melilla* (108 pp.). Fundación Biodiversidad.

Ocaña, O., Betti, F., Garrabou, J., Bo, M., & Terrón-Sigler, A. et al. (2015). *Astroides calycularis. The IUCN Red List of Threatened Species*.

Ocaña, O., Ramos, A., & Templado, J. (2009). *Paisajes sumergidos de la región de Ceuta y su biodiversidad* (254 pp.). Edita Fundación Museo del Mar.

Otero, M. M., Numa, C., Bo, M., Orejas, C., Garrabou, J., Cerrano, C., Kružičãl, P., Antoniadou, C., Aguilar, R., Kipson, S., Linares, C., Terrón-Sigler, A., Brossard, J., Kersting, D., Casado-Ameza, P., Garca, S., Goffredo, S., Ocaa, O., Caroselli, E., … Özalp, B. (2017). *Overview of the conservation status of Mediterranean anthozoans* (73 pp.). IUCN.

Palumbi, S. R. (2004). Marine reserves and ocean neighborhoods: The spatial scale of marine populations and their management. *Annual Review of Environment and Resources*, 29, 31–68. https://doi.org/10.1146/annurev.energy.29.062403.102254

Pelletier, F., Garant, D., & Hendry, A. P. (2009). Eco-evolutionary dynamics. *Philosophical Transactions of the Royal Society of London. Series B, Biological Sciences*, *364*, 1483–1489. https://doi.org/10.1098/rstb.2009.0027

Pellón, J., & Badalamenti, F. (2016). Tentacular release of planulae in Anthozoa: The case of the Mediterranean endemic orange coral *Astroides calycularis* (Scleractinia: Dendrophylliidae). *Coral Reefs*, *35*, 1369. https://doi.org/10.1007/s00338-016-1476-2

Petit, R. J., El Mousadik, A., & Pons, O. (1998). Identifying populations for conservation on the basis of genetic markers. *Conservation Biology*, *12*, 844–855. https://doi.org/10.1046/j.1523-1739.1998.96489.x

Pironon, S., Papuga, G., Villellas, J., Angert, A. L., García, M. B., & Thompson, J. D. (2017). Geographic variation in genetic and demographic performance: New insights from an old biogeographical paradigm. *Biological Reviews*, *92*, 1877–1909. https://doi.org/10.1111/brv.12313

Piry, S., Alapetite, A., Cornuet, J.-M., Paetkau, D., Baudouin, L., & Estoup, A. (2004). GeneClass2: A software for genetic assignment and first-generation migrant detection. *Journal of Heredity*, *95*, 536–539. https://doi.org/10.1093/jhered/esh074

Post, D. M., & Palkovacs, E. P. (2009). Eco-evolutionary feedbacks in community and ecosystem ecology: Interactions between the ecological theatre and the evolutionary play. *Philosophical Transactions of the Royal Society of London. Series B, Biological Sciences*, *364*, 1629–1640. https://doi.org/10.1098/rstb.2009.0012

Prada, F., Musco, L., Alagna, A., Agnetta, D., Beccari, E., D'Anna, G., Giacalone, V. M., Pipitone, C., Vega Fernández, T., Goffredo, S., & Badalamenti, F. (2019). Anthropogenic impact is negatively related to coral health in Sicily (Mediterranean Sea). *Scientific Reports*, *9*, 13469. https://doi.org/10.1038/s41598-019-49713-w

Pritchard, J. K., Stephens, M., & Donnelly, P. (2000). Inference of population structure using multilocus genotype data. *Genetics*, *155*, 945–959. https://doi.org/10.1093/genetics/155.2.945

R Core Team. (2021). *R: A language and environment for statistical computing*. R Foundation for Statistical Computing. Retrieved from https://www.R-project.org/

Rannala, B., & Mountain, J. L. (1997). Detecting immigration by using multilocus genotypes. *Proceedings of the National Academy of Sciences of the United States of America*, *94*, 9197–9201. https://doi.org/10.1073/pnas.94.17.9197

Raymond, M., & Rousset, F. (1995). An exact test for population differentiation. *Evolution*, *49*, 1280. https://doi.org/10.2307/2410454

Reusch, T. B. H., Ehlers, A., Hämmerli, A., & Worm, B. (2005). Ecosystem recovery after climatic extremes enhanced by genotypic diversity. *Proceedings of the National Academy of Sciences of the United States of America*, *102*, 2826–2831. https://doi.org/10.1073/pnas.0500008102

Riginos, C., Hock, K., Matias, A. M., Mumby, P. J., Oppen, M. J. H., & Lukoschek, V. (2019). Asymmetric dispersal is a critical element of concordance between biophysical dispersal models and spatial genetic structure in Great Barrier Reef corals, (E. Treml, Ed.). *Diversity and Distributions*, *25*, 1684–1696. https://doi.org/10.1111/ddi.12969

Roberts, C. M., O'Leary, B. C., McCauley, D. J., Cury, P. M., Duarte, C. M., Lubchenco, J., Pauly, D., Sáenz-Arroyo, A., Sumaila, U. R., Wilson, R. W., Worm, B., & Castilla, J. C. (2017). Marine reserves can mitigate and promote adaptation to climate change. *Proceedings of the National Academy of Sciences of the United States of America*, *114*, 6167–6175. https://doi.org/10.1073/pnas.1701262114

Rousset, F. (1997). Genetic differentiation and estimation of gene flow from F-statistics under isolation by distance. *Genetics*, *145*, 1219–1228.

Rousset, F. (2008). genepop'007: A complete re-implementation of the genepop software for Windows and Linux. *Molecular Ecology Resources*, *8*, 103–106. https://doi.org/10.1111/j.1471-8286.2007.01931.x

Rousset, F., Beeravolu, C. R., & Leblois, R. (2018). Likelihood analysis of population genetic data under coalescent models: Computational and inferential aspects. *Journal de la Société Française de Statistiques*, *159*, 142–166.

Sagarin, R. D., & Gaines, S. D. (2002). The "abundant centre" distribution: To what extent is it a biogeographical rule? *Ecology Letters*, *5*, 137–147. https://doi.org/10.1046/j.1461-0248.2002.00297.x

Schoener, T. W. (2011). The newest synthesis: Understanding the interplay of evolutionary and ecological dynamics. *Science*, *331*, 426–429. https://doi.org/10.1126/science.1193954

Sexton, J. P., McIntyre, P. J., Angert, A. L., & Rice, K. J. (2009). Evolution and ecology of species range limits. *Annual Review of Ecology Evolution and Systematics*, *40*, 415–436. https://doi.org/10.1146/annurev.ecolsys.110308.120317

Slatkin, M., & Excoffier, L. (2012). Serial founder effects during range expansion: A spatial analog of genetic drift. *Genetics*, *191*, 171–181. https://doi.org/10.1534/genetics.112.139022

Sorgente, R., Olita, A., Oddo, P., Fazioli, L., & Ribotti, A. (2011). Numerical simulation and decomposition of kinetic energy in the Central Mediterranean: Insight on mesoscale circulation and energy conversion. *Ocean Science*, *7*, 503–519. https://doi.org/10.5194/os-7-503-2011

Sun, J. X., Helgason, A., Masson, G., Ebenesersdóttir, S. S., Li, H., Mallick, S., Gnerre, S., Patterson, N., Kong, A., Reich, D., & Stefansson, K. (2012). A direct characterization of human mutation based on microsatellites. *Nature Genetics*, *44*(10), 1161–1165. https://doi.org/10.1038/ng.2398

Szpiech, Z. A., Jakobsson, M., & Rosenberg, N. A. (2008). ADZE: A rarefaction approach for counting alleles private to combinations of populations. *Bioinformatics*, *24*, 2498–2504. https://doi.org/10.1093/bioinformatics/btn478

Teixidó, N., Caroselli, E., Alliouane, S., Ceccarelli, C., Comeau, S., Gattuso, J.-P., Fici, P., Micheli, F., Mirasole, A., Monismith, S. G., Munari, M., Palumbi, S. R., Sheets, E., Urbini, L., De Vittor, C., Goffredo, S., & Gambi, M. C. (2020). Ocean acidification causes variable trait-shifts in a coral species. *Global Change Biology*, *26*, 6813–6830. https://doi.org/10.1111/gcb.15372

Templado, J., Calvo, M., Luque, A., Garvia, A., Maldonado, M. et al. (2004). *Guia de los invertebrados y peces marinos españoles protegidos por la legislacion nacional e internacional*. Ministerio de Medio Ambiente.

Terrón-Sigler, A., León-Muez, D., Peñalver-Duque, P., & Torre, F. E. (2016). The effects of SCUBA diving on the endemic Mediterranean coral *Astroides calycularis*. *Ocean and Coastal Management*, *122*, 1–8. https://doi.org/10.1016/j.ocecoaman.2016.01.002

Torrents, O., Tambutté, E., Caminiti, N., & Garrabou, J. (2008). Upper thermal thresholds of shallow vs. deep populations of the precious Mediterranean red coral *Corallium rubrum* (L.): Assessing the potential effects of warming in the NW Mediterranean. *Journal of Experimental Marine Biology and Ecology*, *357*, 7–19. https://doi.org/10.1016/j.jembe.2007.12.006

Weir, B. S., & Cockerham, C. C. (1984). Estimating F-statistics for the analysis of population structure. *Evolution*, *38*, 1358. https://doi.org/10.2307/2408641

Yakimowski, S. B., & Eckert, C. G. (2007). Threatened peripheral populations in context: Geographical variation in population frequency and size and sexual reproduction in a clonal woody shrub. *Conservation Biology*, *21*, 811–822. https://doi.org/10.1111/j.1523-1739.2007.00684.x

Zibrowius, H. (1980). Les scléractiniaires de la Méditerranée et de l'Atlantique nord-oriental. *Mémoires de L'institut Océanographique*, *11*, 284.

Zibrowius, H. (1995). The "Southern" *Astroides calycularis* in the Pleistocene of the northern Mediterranean—An indicator of climatic changes (Cnidaria, scleractinia). *Geobios*, *28*, 9–16. https://doi.org/10.1016/S0016-6995(95)80201-0

BIOSKETCH

JBL, PLS, DGG and CL belong to the research group MedRecover (https://medrecover.org) led by JG at the Institute of Marine Science (ICM-CSIC) in Barcelona, Spain. The group is focused on the conservation biology of Mediterranean rocky benthic communities and develops complementary approaches from population genetics to community ecology. JBL is affiliated to the Interdisciplinary Centre of Marine and Environmental Research (CIIMAR; http://CIIMAR.up.pt/) in Porto, Portugal. He is focused on the eco-evolution of temperate corals in the context of climate change, combining population genetics, genomics and experimental ecology.

Author contributions: J.B.L, J.B.S and J.G conceived the study. J.B.L, R.G, C.L, O.O, D.G.G and J.G collected the samples. J.B.L, P.L.S, M.H and V.R.S performed the DNA laboratory work. J.B.L, M.H and R.L analysed the genetic data. J.B.L wrote the paper with inputs from all co-authors.

SUPPORTING INFORMATION

Additional supporting information may be found online in the Supporting Information section.